Lecture 15 September 2016

National Research Nuclear University MEPhI, Moscow Russia.

High Resolution X-Ray Spectromicroscopy of Laser Produced Plasmas

Faenov A.Ya.

Institute for Academic Initiatives, Osaka University Japan

and

Joint Institute for High Temperature of

Russian Academy of Science, Russia

OUTLINE

Short introduction

Information, which gives X-Ray spectroscopy of multicharged ions about plasma, created by laser pulses Types of targets and typical laser parameters Satellite structures of multicharged ions. Features of X-Ray spectra, obtained in ns, ps and fs plasma.

X-ray spectroscopic and imaging techniques

Different types of X-Ray spectrometers
1) Focusing Spectrometers with Spatial Resolution (FSSR-1,2D)

2) X-ray monochromatic backlighting and self imaging with high spatial resolution and big field of view.

High resolution X-ray spectromicroscopy of diferent laser plasma

Comparison of high resolution X-Ray spectra from various laser plasma sources

Applications of High-resolution X-Ray spectromicroscopy

1970

Nanosecond lasers

τ_{las} = 1÷ 100 ns

E_{las} = 0.001 ÷ 100 kJ

I_{las} = 10^{12} ÷ 10^{16} W/cm ^{2}

1980

Picosecond lasers

τ_{las} = 1÷ 300 ps

E_{las} = 1÷ 1000 J

I_{las} = 10^{14} ÷ 10^{19} W/cm ^{2}

1990

Femtosecond lasers

τ_{las} = 20 ÷ 500 fs

E_{las} = 0.01÷ 50 J

I_{las} = 10^{16} ÷ 10^{21} W/cm ^{2}

2000

Ultra-intense X-ray free electron lasers (XFEL)

2010

I_{las} = 10^{16} ÷ 10^{21} W/cm ^{2}

Laser plasma radiation

- **Atomic Physics and X-Ray spectroscopy of multicharged ions**
- **Plasma diagnostic**
- **Verification of numerical plasma models**
- **Creation of X-ray radiation sources**
- **X-ray photoionization of matter. Creation exotic states. Diagnostics of warm dense plasma**

Types of targets used in laser plasma experiments

Solid

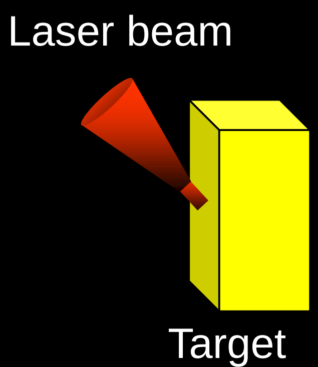

Clusters

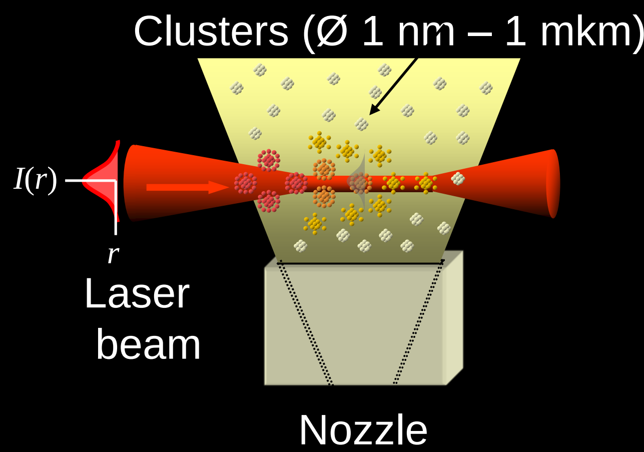

Porous

Aerogel dust
(particles Ø 5-500 μm with density 0.04 – 0.1 g/cm^3)

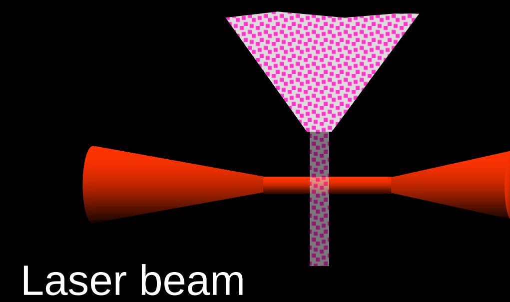

ZNIIMASH, Korolev, Moscow reg., Russia

Hebrew University, Jerusalem, Israel

Los Alamos National Laboratory, USA

Livermore National Laboratory, USA

Saclay Laboratory, CEA, France

CELIA, Bordeaux University, France

KPSI, JAEA, Japan

RAL, UK

University of Maryland, USA

GSI, Germany

ENEA and Tor Vergata University, Italy

Laser pulse:

$\lambda = 0.25 - 1\ \mu m$

$E = 1\ mJ - 300\ J$

$\tau = 20\ fs - 100\ ns$

$I_{las} = 10^{11} - 10^{21}\ W/cm^2$

$f = 0.01 - 20\ Hz$

Advantages of cluster targets

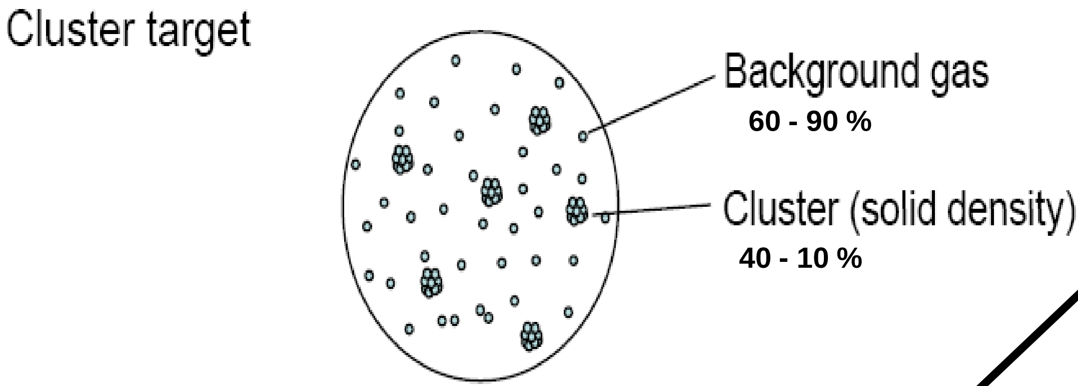

Clusters (Ø 1 nm – 1 μm, N_{atoms} up to 10^9)

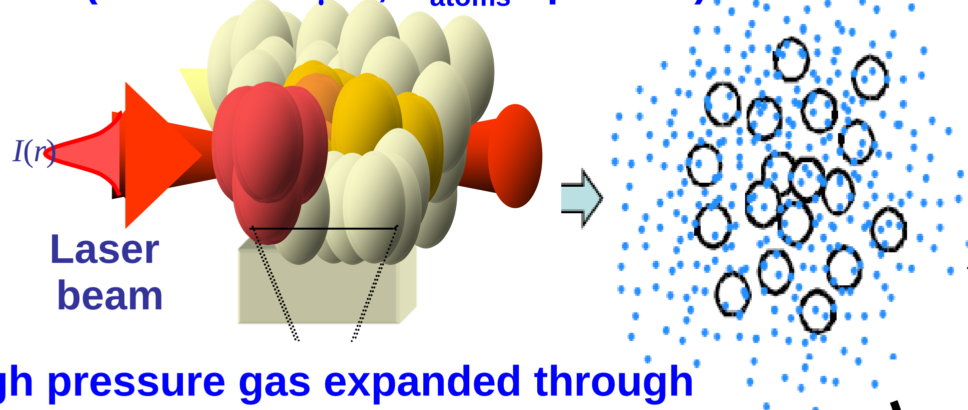

High pressure gas expanded through supersonic gas nozzle

Energetic electrons 600 MeV
10 TW, Ti:Sa laser, 100 fs,1 J, Ar clusters
Zhang L. et al., Appl. Phys. Lett. 100, 014104 (2012)

X-ray photons :

Monoch. hν~ 0.65 keV, 2.8×10^{10} ph/pulse
4 TW, Ti:Sa laser, 40 fs,150 mJ, 90%He+10%CO_2 clusters
Fukuda Y. et al., Apl. Phys. Lett., 103, 165002 (2009)

hν~ 3 keV, 2.5×10^{11} ph/pulse (η~ 1.2×10^{-4})
hν~ 12.7 keV, 8×10^{8} ph/pulse (η~ 1.6×10^{-6})
4 TW, Ti:Sa laser, 40 fs,150 mJ, Ar and Kr clusters
Zhang L. et al., Optics Express, 100, 014104 (2012)

hν~ 30 keV, 3.1×10^{7} ph/pulse (η~ 1.5×10^{-7})
25 TW, Ti:Sa laser, 40 fs,1 J, Xe clusters
Hayashi Y. et al., Opt. Lett., 36, 1614 (2011)

10-20 MeV/n fast ions
4 TW, Ti:Sa laser, 40 fs,150 mJ, 90%He+10%CO_2 clusters
Fukuda Y. et al., Phys. Rev. Lett., 103, 165002 (2009)

5.5×10^{6} D-D neutrons
100 TW, Ti:Sa laser, 50 fs,5.4 J, CD_4 clusters
Lu H.Y.. et al., Phys. Rev. A, 80, 051201 (R) 100, 014104 (2009)

Advantages:

- **High absorption of laser radiation**
- **Less debris => No optics damage**
- **Fast refresh => High average power**
- **Suitable for many applications**

Low background noise

General parameters of laser-produced plasma, measured by X-ray spectromicroscopy methods

Bulk electron temperature:
$T_e = 10 \div 4000$ eV

Electron density :
$N_e = 10^{18} \div 10^{24}$ см$^{-3}$

Ions charge state:
$Z_i > 5$

Ionization potential
$E_i > 0.5$ keV

Spectra of
H-; He-; Ne-; Ni-like ions and their dielectronic satellites
Spectral range:
$\lambda \leq 20$ Å

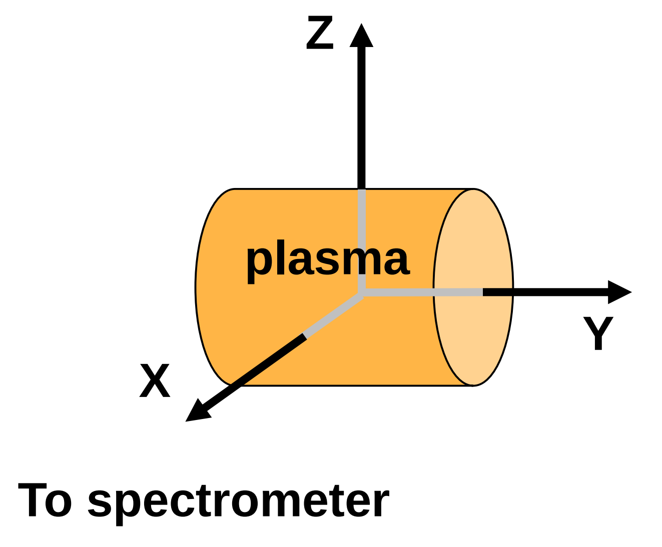

Observed quantity:

$$S_{obs}(\lambda, y, t) = \iint S(\lambda, x, y, z, t)\,dxdz$$

(film, Image plate or CCD is used for registration)

$$S_{obs}(\lambda, y) = \iiint S(\lambda, x, y, z, t)\,dxdzdt$$

where $S(\lambda,x,y,z,t)$ – emission plasma spectrum from the region (x,y,z) at time t

Quantity $S(\lambda,x,y,z,t)$ is calculated with the help of some kinetic model of plasma. It can depend on different plasma parameters, which define its emission properties:

-N_e, T_e, T_i, ionization state N_{Z+1}/N_Z $(Z=1,\ldots,Z_{nucl})$

-N_e^{hot}, T_e^{hot} – if electrons are not Maxwellian and fraction of hot electrons presents

-N_i^{hot}, T_i^{hot} - if ions are not Maxwellian and fraction of hot ions presents

-L – plasma size (if optical thickness is important)

- H_{qs}, E_{qs}, E_{osc}, H_{osc}, ω_{osc} – strengths of quasistatic electrical or magnetic fields and frequency of oscillating fields

Comparison of observed $S_{obs}(\lambda, y)$ with calculated one

$$S_{\mathrm{mod}}(\lambda, y) = \iiint S(\lambda, x, y, z, t)\, dxdzdt$$

allows to determine plasma parameters averaged on *x,z,t*

If spectral resolution of spectrometer is enough high then observed function $S_{obs}(\lambda, y)$ includes information on both intensities and profiles of various spectral lines

It is possible to diagnose such plasma parameters as strengths of electrical and magnetic fields, ion density and temperature and plasma expansion velocity, which effect mainly on spectral line profiles

As a rule plasma is *very inhomogeneous*, and some processes occur only in a narrow spatial plasma regions

observation of such processes is possible only if spectrometer has a very good spectral and spatial resolution (in some cases observation of plasma from different directions can be necessary)

Electron impact excitation

Atomic structure of H-like ions and their dielectronic satellites

Radiative transitions

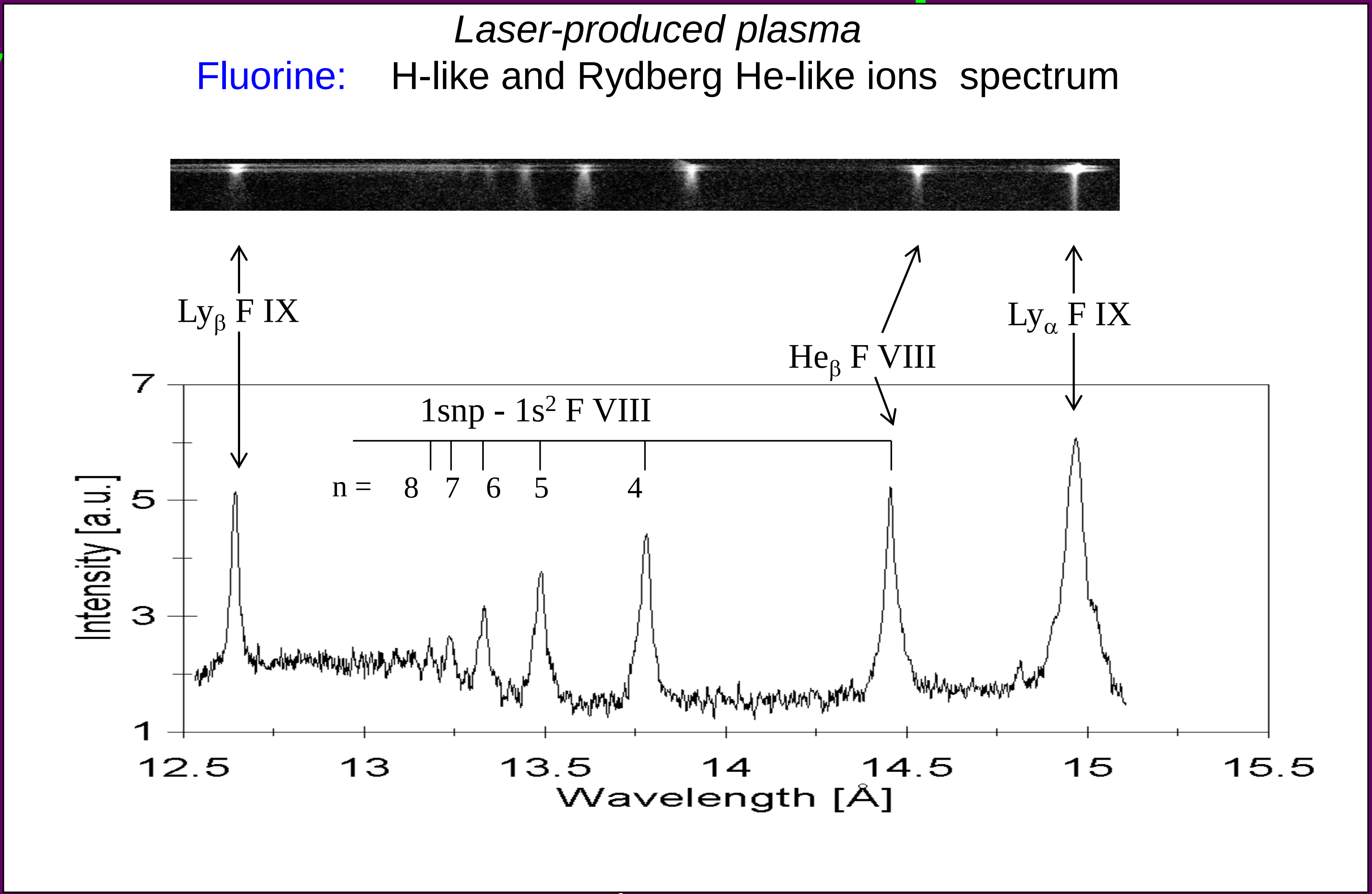

Inner-shell exitation $1s2l+e \rightarrow 2l3l' + e \rightarrow$ $\begin{cases} 1s3l + h\omega\ (Ly_\alpha) \\ 1s2l + h\omega'\ (Ly_\beta) \end{cases}$

Ly_α Si XIV spectrum is very depend from the laser plasma conditions

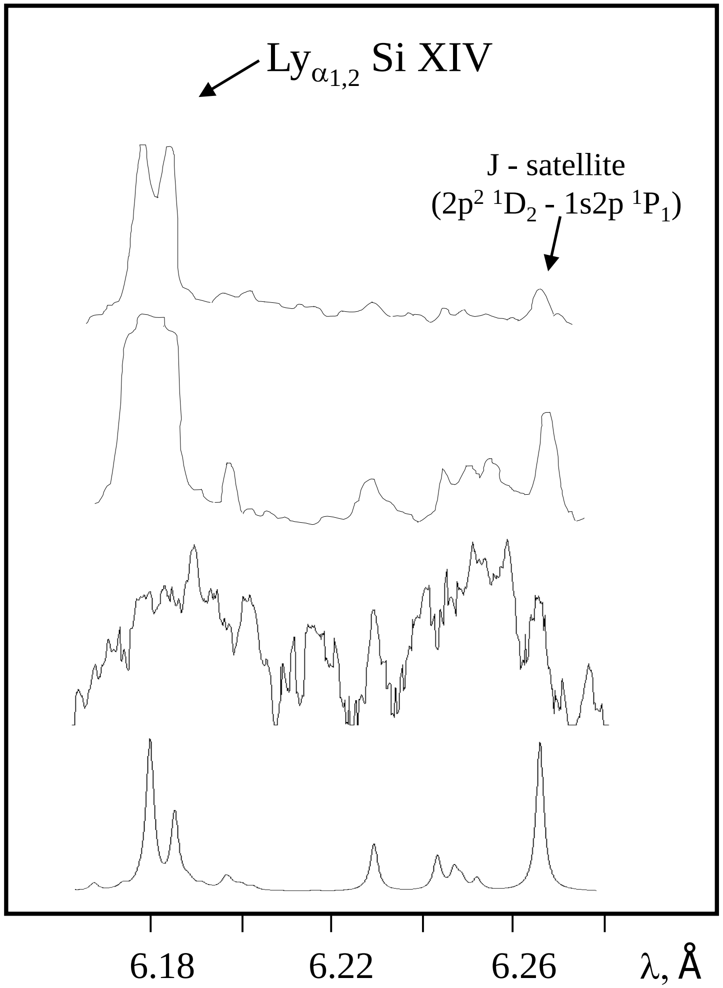

← **Nanosecond laser plasma**

← **Picosecond laser plasma**

← **Femtosecond laser plasma (high contrast)**

← **Coronal model**

Intensities of satellite lines depend of plasma parameters

I. Low dense plasma (coronal approximation)

Resonance lines

$$I_R^Z \sim N_0^Z N_e \langle v\sigma^{ex}_{0R} \rangle + N_0^{Z+1} N_e \langle v\sigma^{ph}_{0R} \rangle + N_0^{Z-1} N_e \langle v\sigma^{ion}_{0R} \rangle$$

$\langle v\sigma^{ex}_{0R} \rangle$ - rate of electron impact excitation

$\langle v\sigma^{ph}_{0R} \rangle$ - rate of photorecombination

$\langle v\sigma^{ion}_{0R} \rangle$ - rate of electron impact ionization

N_0^Z, N_0^{Z+1}, N_0^{Z-1} – ground state populations of ions Z, Z+1 and Z-1

N_e – electron plasma density)

Satellite lines

$$I_S^{Z-1} \sim \left(N_0^Z N_e \langle v\sigma^{dc}_{0S} \rangle + N_0^{Z-1} N_e \langle v\sigma^{ex}_{0S} \rangle \right) A_{SI} / \left(\Gamma_S + \Sigma A_{SI} \right)$$

$\langle v\sigma^{dc}_{0S} \rangle$ - rate of dielectronic capture

$\langle v\sigma^{ex}_{0S} \rangle$ - rate of electron impact excitation)

Low dense plasma (coronal approximation)

Usually, $N_0^Z\langle v\sigma^{ex}{}_{0R}\rangle$ >> $N_0^{Z+1}\langle v\sigma^{ph}{}_{0R}\rangle$, $N_0^{Z-1}\langle v\sigma^{ion}{}_{0R}\rangle$;

in this case:

$$I_S^{Z-1}/I_R^Z \sim A_{SI}/(\Gamma_S + \Sigma A_{SI})\{\langle v\sigma^{dc}{}_{0S}\rangle/\langle v\sigma^{ex}{}_{0R}\rangle + (N_0^{Z-1}/N_0^Z)\langle v\sigma^{ex}{}_{0S}\rangle/\langle v\sigma^{ex}{}_{0R}\rangle\}$$

1) $A_{SI} \sim Z^4$, $\Gamma_S \sim$ const $\rightarrow$ if $Z \rightarrow 1$, $A_{SI} / (\Gamma_S + \Sigma A_{SI}) \rightarrow 10^{-5}$
if $Z \rightarrow \infty$, $A_{SI} / (\Gamma_S + \Sigma A_{SI}) \rightarrow 1$,

i.e. satellites are intensive for multicharged ions and are small for neutral atoms

2) $\langle v\sigma^{dc}{}_{0S}\rangle / \langle v\sigma^{ex}{}_{0R}\rangle \sim \exp((E_R-E_S)/kT_e)$,

$(N_0^{Z-1}/N_0^Z)\langle v\sigma^{ex}{}_{0S}\rangle / \langle v\sigma^{ex}{}_{0R}\rangle \sim \exp((E_0^Z-E_0^{Z-1})/kT_e)$

$E_R > E_S$, $E_0^Z > E_0^{Z-1}$

i.e. satellites are intensive in relatively cold plasma

Low dense plasma (coronal approximation)

Summary

Satellites are intensive for large Z and small T_e.

More exactly, parameter T_e/Z^2 (because of all energies are proportional to Z^2) must be small.

It means that in multicharged plasma satellites may be intensive even at relatively high temperatures.

Super high density plasma (LTE-approximation)

$$I_S^{Z-1}/I_R^Z \sim N_e\,(A_{SI}/A_R)\exp\left(\left(E_R - E_S\right)/kT_e\right)$$

When N_e increases and T_e decreases → Satellite relative intensities increase

For Z ~ 10 LTE-approximation is valid only in super dense plasma with $N_e \gg 10^{23}$ cm^{-3}.

Dense plasma (intermediate case)
short wavelengths ns-, ps-, fs- laser-produced plasma

For Z ~10-20 this case corresponds to plasma

with 10^{20} cm^{-3} < N_e < 10^{24} cm^{-3}

No simple approximations!

Numerical solving of large system

of collisional-radiative kinetic equations is needed

to define satellite line intensities

Intensities of satellite lines depend of plasma parameters

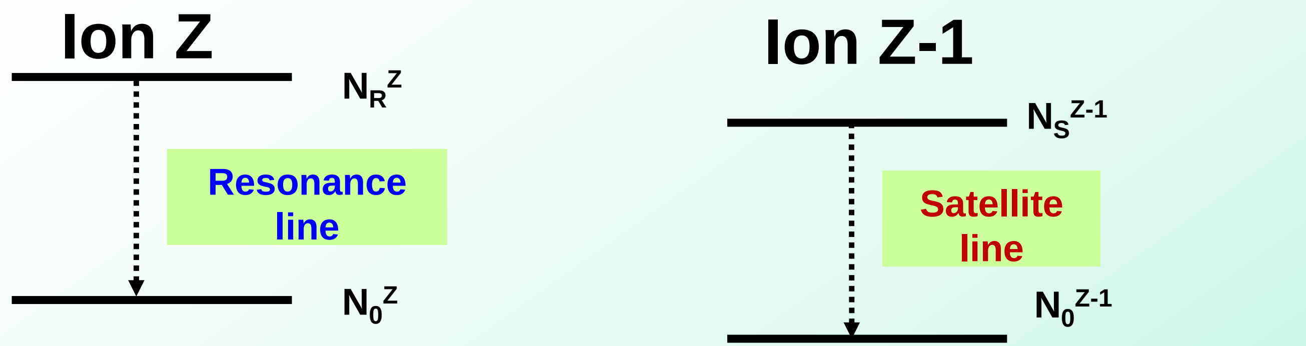

$$I_R^Z = A_R N_R^Z$$

intensity of resonance line

$$I_S^{Z-1} = A_S N_S^{Z-1}$$

intensity of satellite line

N_R^Z, N_S^{Z-1} – *population of resonance and satellite levels*

Intensity of resonance line depends from : rate of electron impact excitation, rate of photorecombination, rate of electron impact ionization, ground state populations of ions Z, Z+1 and Z-1, electron plasma temperature and density

A_R, A_{SI} – *probabilities of radiative transitions for resonance and satellite lines*

Intensity of satellite line depends from: rate of dielectronic capture, rate of electron impact excitation, ground state populations of ions Z, Z+1 and Z-1, electron plasma temperature and density

Kinetic analyze of line intensities of Resonance and satellite lines ratio shows that:

1) S**atellites are intensive for multicharged ions of high Z elements and are small for low z elements**
2) Satellites are intensive for colder plasma
3) Satellites are intensive for denser plasma

Atomic structure of He-like ions and their dielectronic satellites

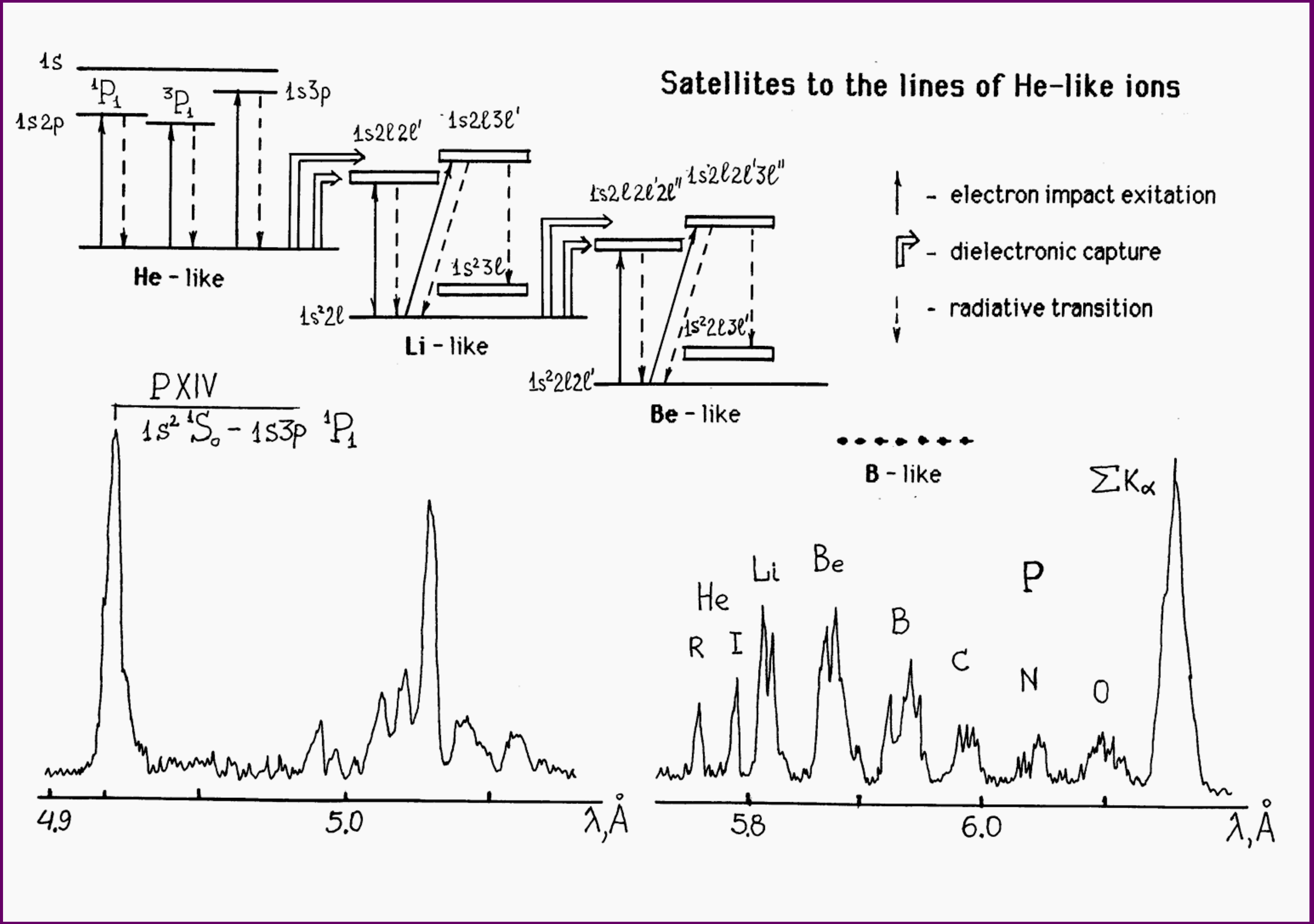

Spectra in the vicinity of He_{α} line is strongly depends from laser plasma conditions

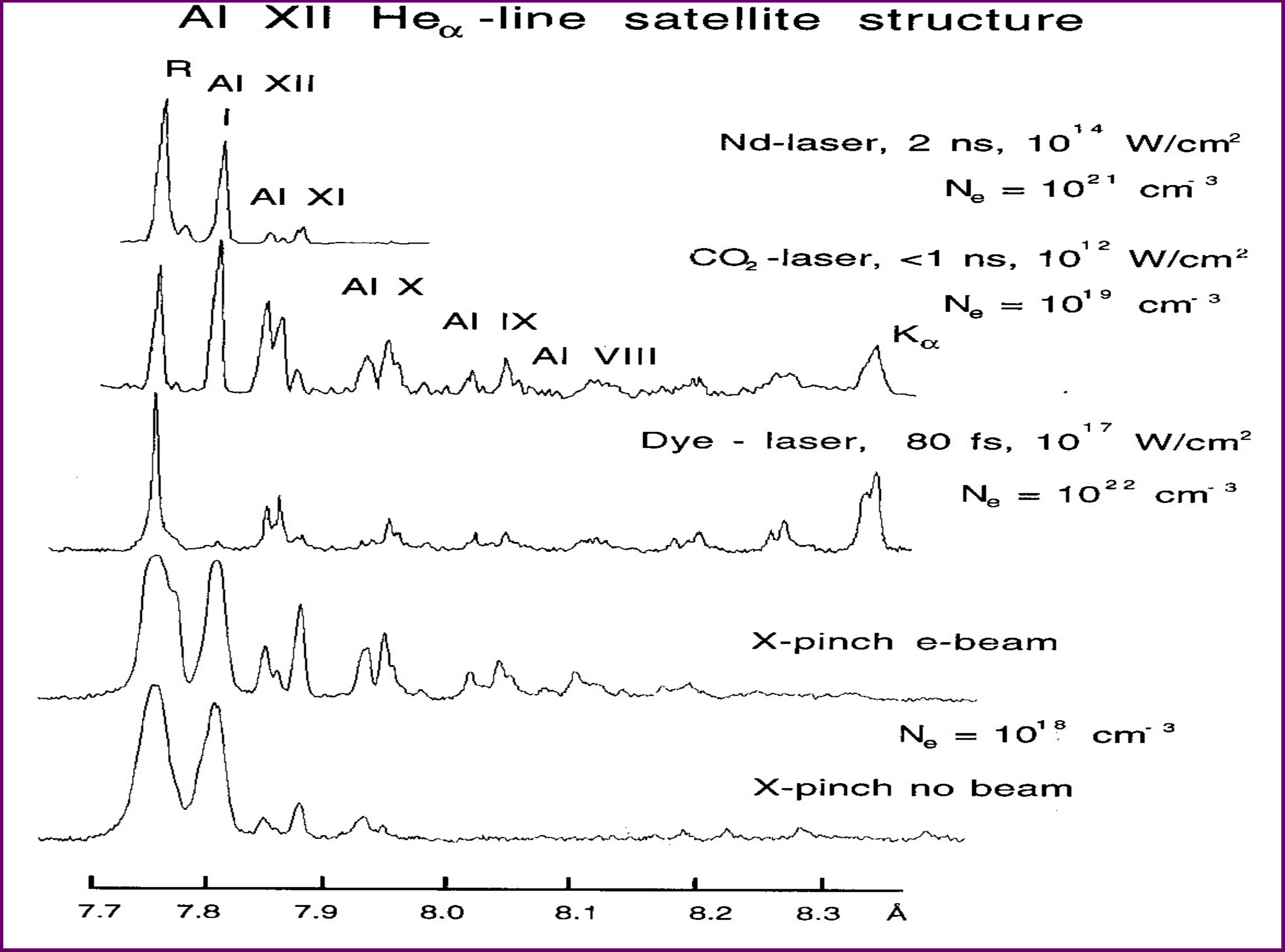

He- like Ar: experimental spectra from different plasma sources

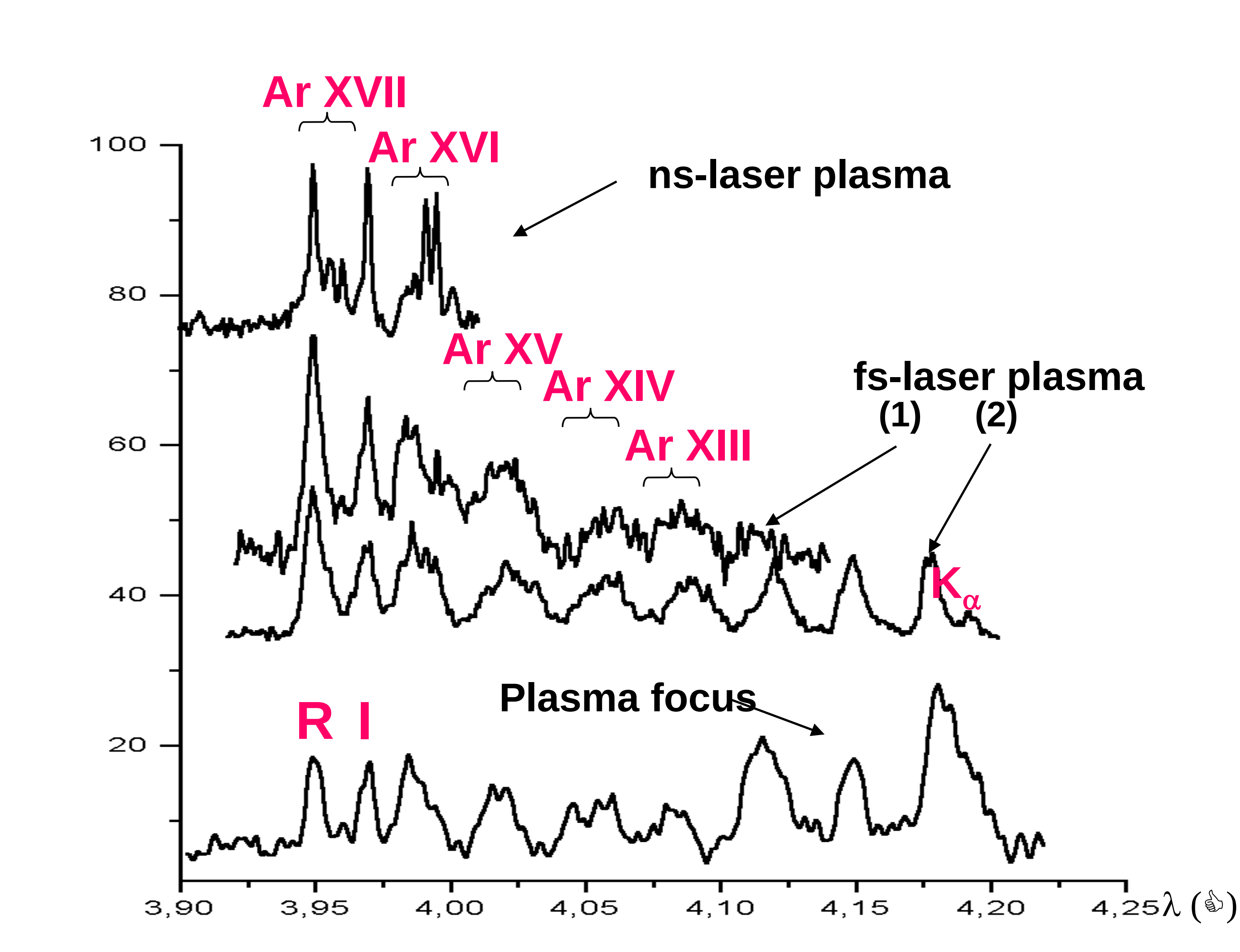

Atomic structure of Ne-like ions and their dielectronic satellites

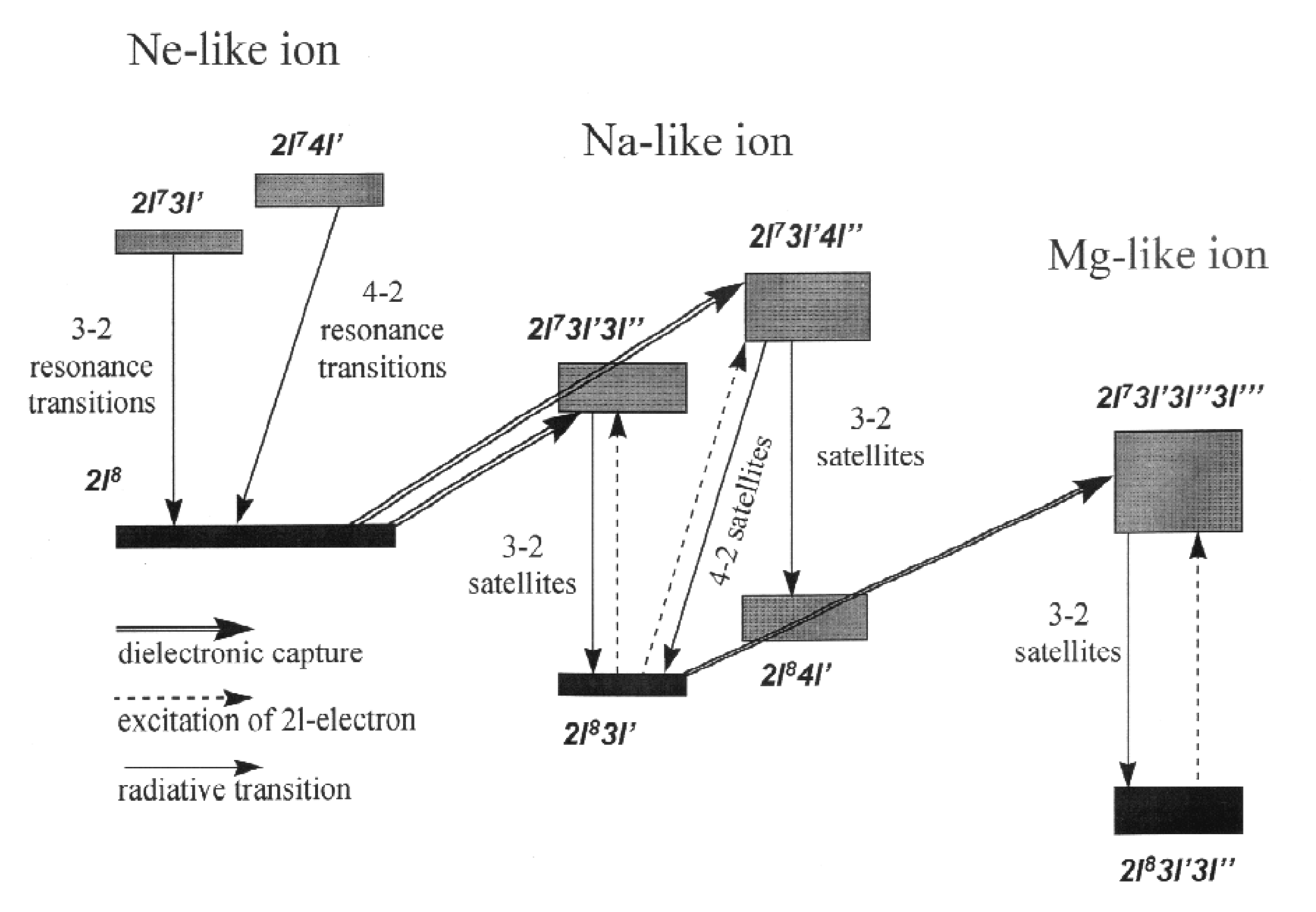

Line profiles near the vicinity of 3-2 resonance lines of Ne-like Fe XVII

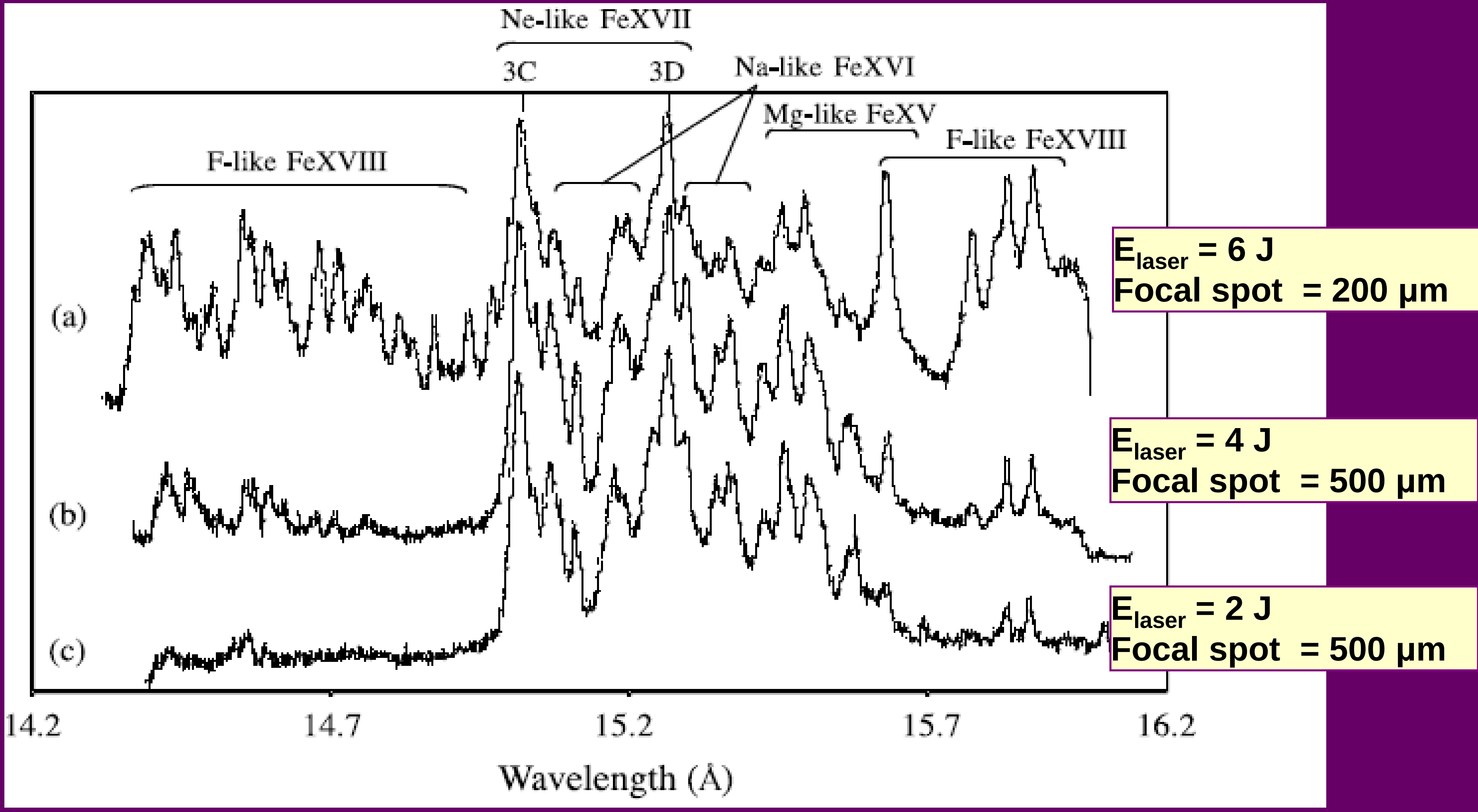

Typical X-ray spectra of Fe between 14 and 16 Å obtained in plasmas produced by the 15 ns Nd:glass laser

(Tor Vergata University, Rome, Italy)

X-ray spectroscopic and imaging techniques

Principals of X- Ray crystal spectroscopy

Different types of X- Ray spectrometers

Focusing Spectrometers with Spatial Resolution (FSSR-1,2D)

X-ray monochromatic backlighting with high spatial resolution and big field of view

High-luminosity X-ray monochromatic self imaging with high spatial resolution and big field of view

X-ray crystal spectroscopy: main principals

Basic condition: Bragg diffraction $m\lambda = 2d \sin \Theta$

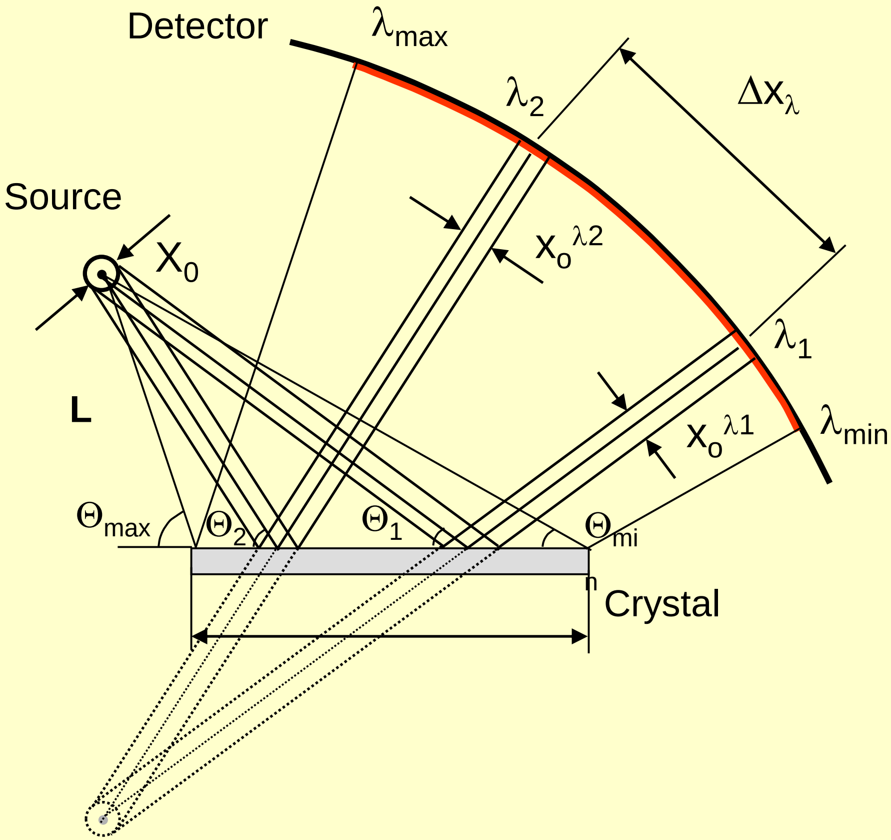

$$\Delta x_\lambda = \frac{\Delta\lambda}{\lambda} L \, tg\Theta$$

$$\frac{\lambda}{\Delta\lambda} = \frac{L}{x_0} tg\Theta$$

$$\lambda_{max} < 2d$$

2d ~ (0.8 ÷ 26) Å
Spectral range (0.5 ÷15) keV

X-ray crystal spectromicroscopy: main parameters

Basic condition: Bragg diffraction $m\lambda = 2d \sin \Theta$

- **Angular dispersion** $D_\theta = \dfrac{d\lambda}{d\theta}$ **or linear dispersion** $D_x = \dfrac{d\lambda}{dx}$

  $D_\theta = \dfrac{2d}{m} \cos\theta = \lambda \operatorname{ctg}\theta$ $\qquad D_x = D_\Theta \dfrac{d\Theta}{dx}$

- **Spectral resolution** $M = \dfrac{\lambda}{\Delta\lambda}$

- **Spectral range** $\Delta\lambda = \lambda_{max} - \lambda_{min}$

- **Luminosity** $\xi = \dfrac{E}{\Phi} = \dfrac{\Phi_1}{S\ \Phi} = \dfrac{\rho\Omega}{S 4\pi}$

- **Spatial resolution**

Obtaining of a spatial resolution (X-ray spectromicroscopy)

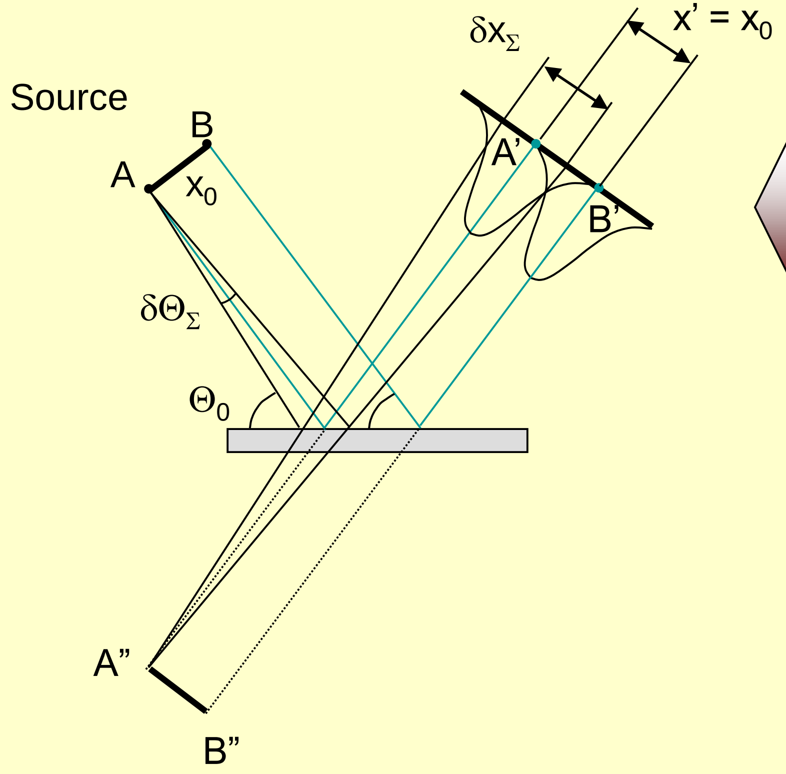

Spatial resolution in the plane of dispersion

Two dimensional spatial resolution

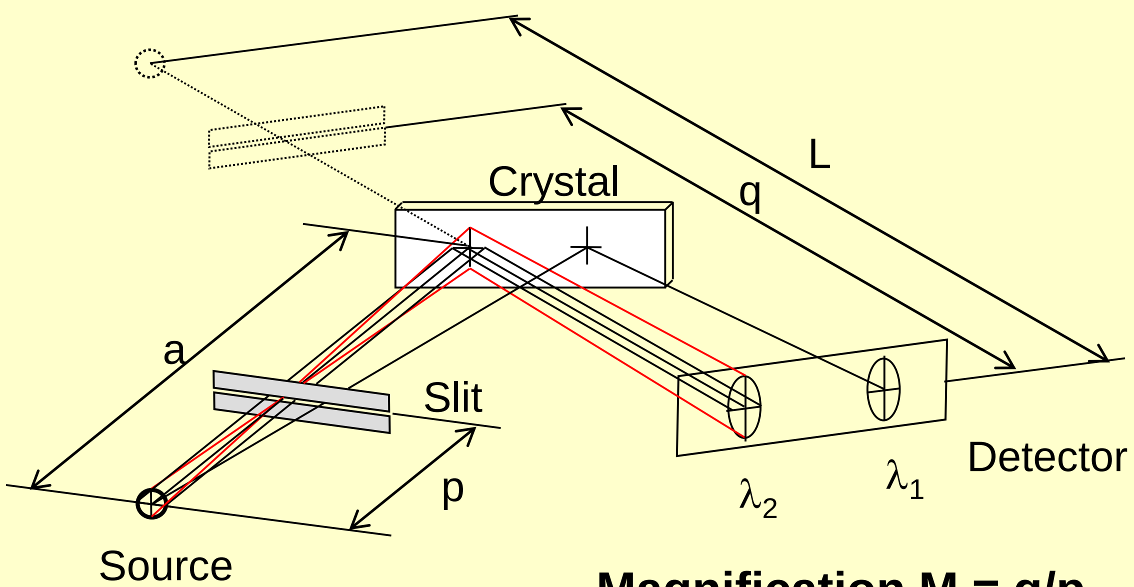

Magnification M = q/p

- Flat crystal
- Cylindrically bent crystal
  - Defocusing spectrometer
  - Iohan & Iohanson spectrometer
  - Hamoshi spectrometer
  - Coshua spectrometer
- Spherically bent crystal
- Elliptical or other second order surface crystals
- Toroidally bent crystal

Focusing spectrometer with spatial resolution (FSSR)

(No slit to obtain spatial resolution!)

FSSR-1D

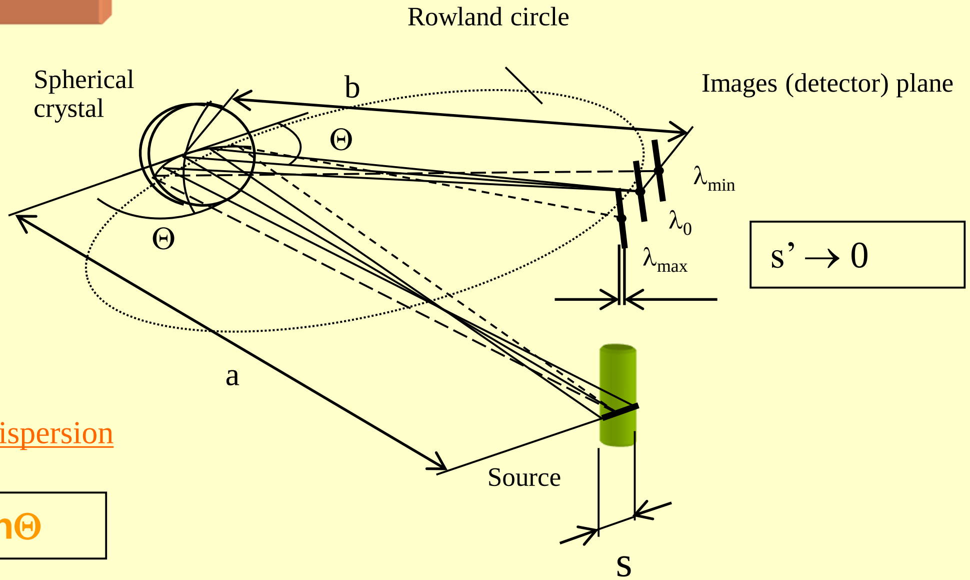

Plane of dispersion

1/a + 1/b =2/RsinΘ

$$a = R\frac{\sin\Theta}{\cos 2\Theta}$$

$$b = R\sin\Theta$$

$$M_s = \cos 2\Theta$$

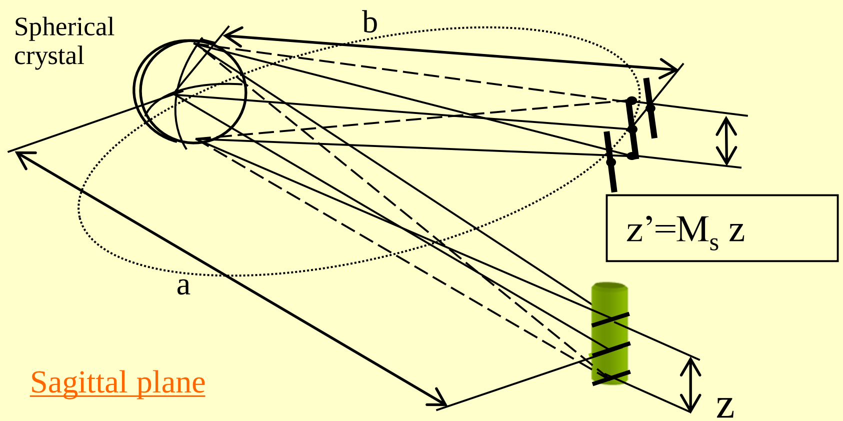

Sagittal plane

Ref.: A.Faenov et al., Physica Scripta, **50**, 333 (1994); I.Skobelev et al., JETP, **81** , 692 (1995);
T.Pikuz et al., J.X-ray Science and Technology, **5**, 517-521 (1995)

View of the experimental vacuum chamber with installed spectrometers (film detector)

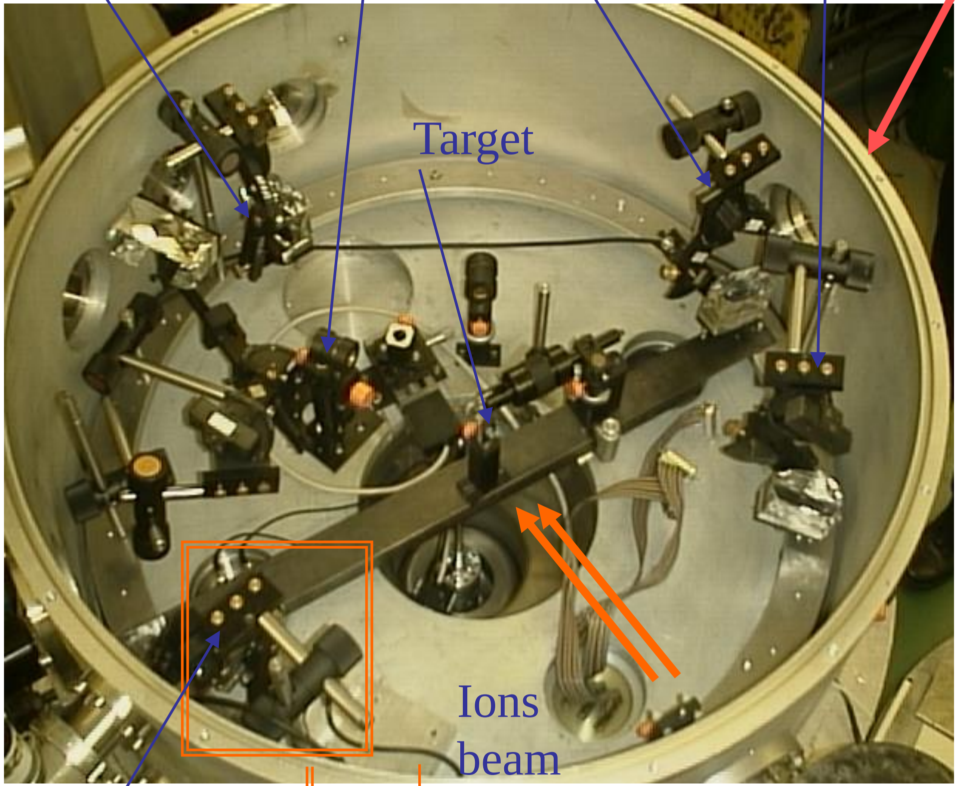

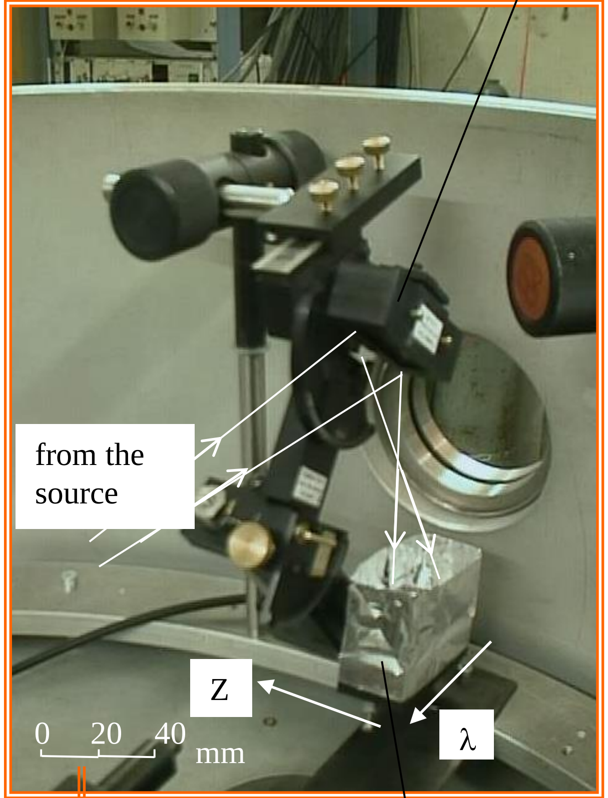

GSI, Germany

Laser installation “Neodim” (ZNIIMASH, Korolev, Russia)

Vacuum chamber with FSSR spectrometer

Vacuum chamber with target

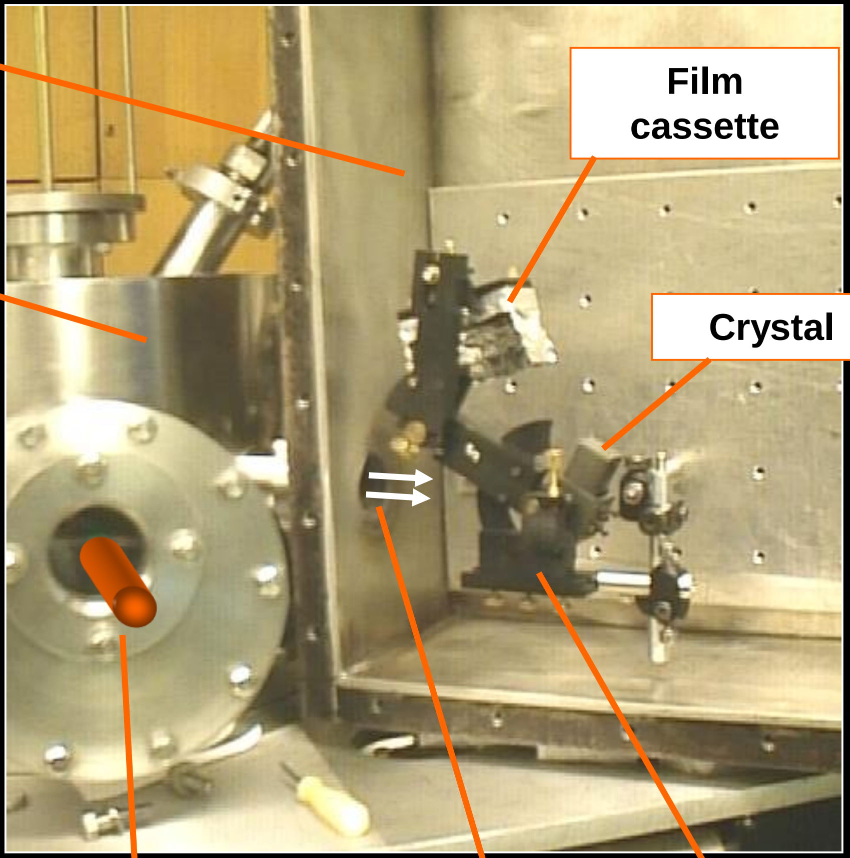

Laser Beam

$E \approx 1.5$ J, $\tau = 1$ пс

$q \approx 3 \times 10^{17}$ W/cm^2

X-ray radiation from plasma

FSSR spectrometer

FSSR could be very easly combined with different detectors

X-ray CCD

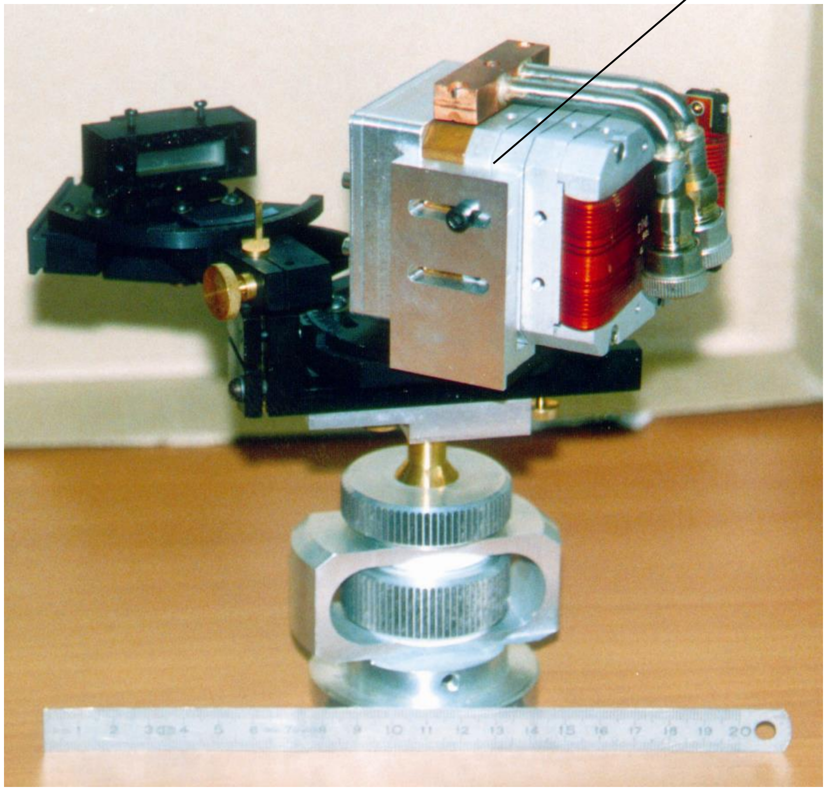

CELIA, Bordeaux University, France

Ref.: F.Blasco et al.,RSI ,**72** (4), 1956-1962 (2001)

MCP

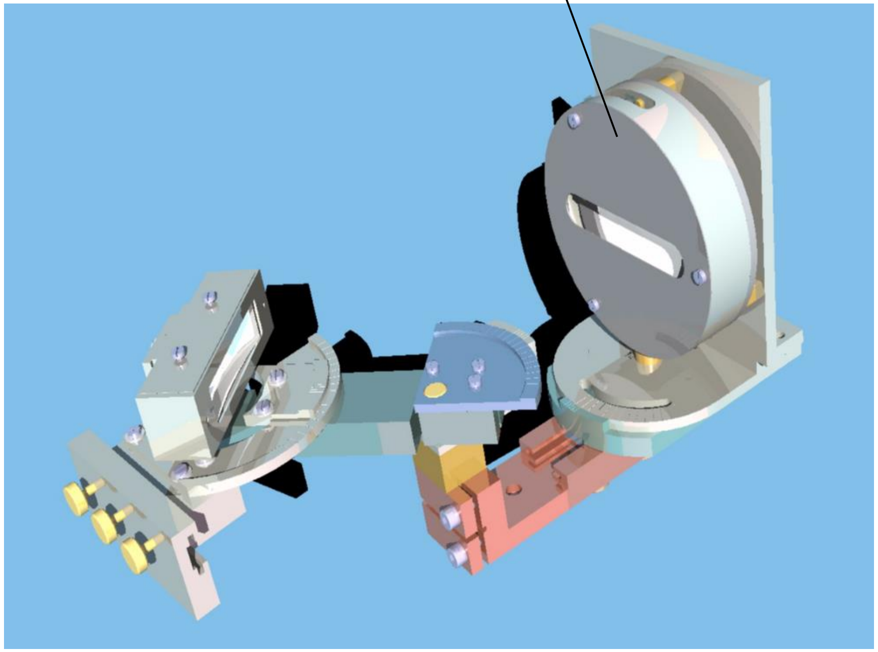

SPAM/DRECAM, Saclay, France

Ref.: P.Monot et al.,NIMA ,**484**, 299-311 (2002)

JAEA (Japan) : Ti:Sa 20 fs laser interaction with clusters

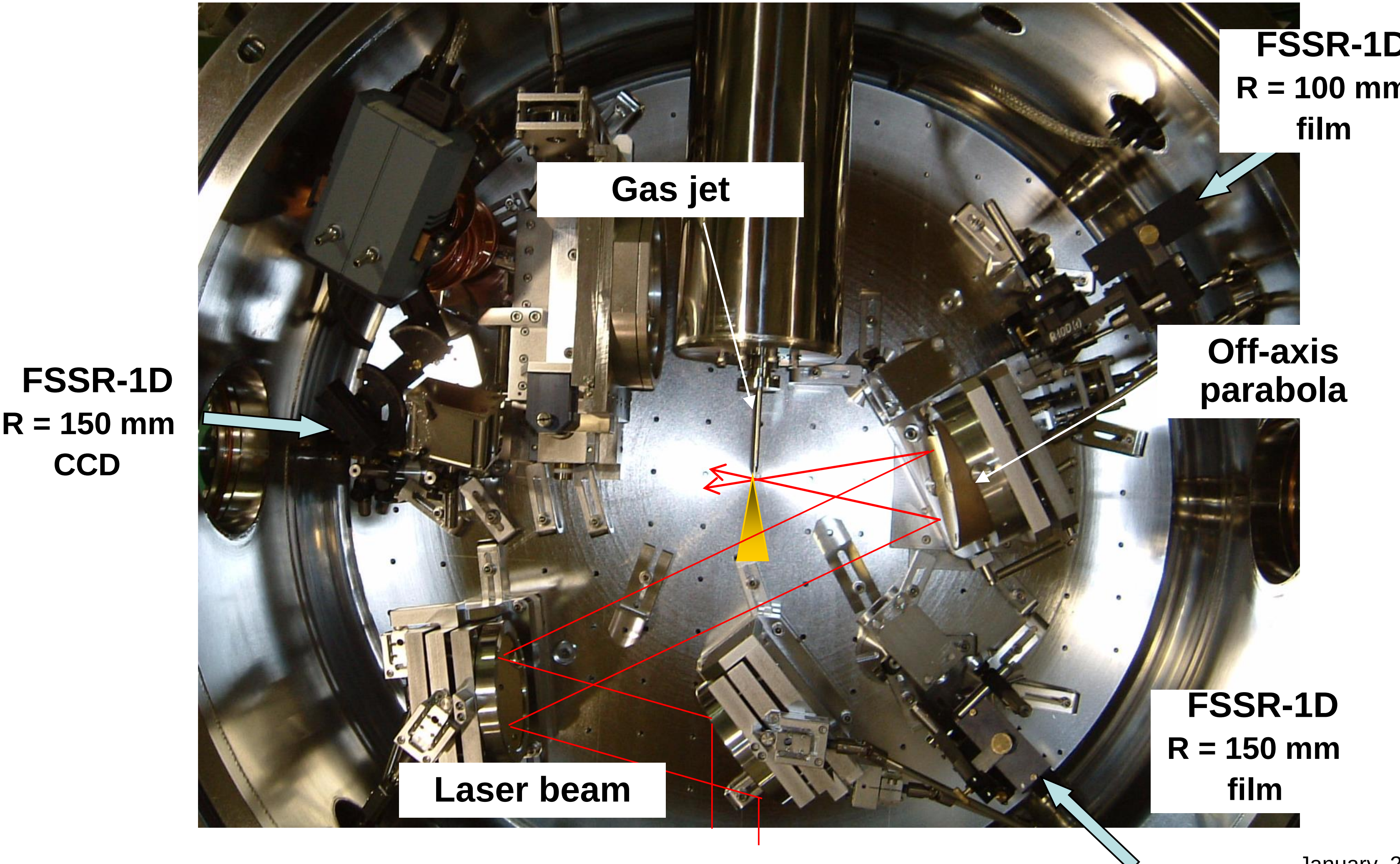

January, 2003

Typical spectrogram with spatial resolution of H- and He-like ions of Oxygen

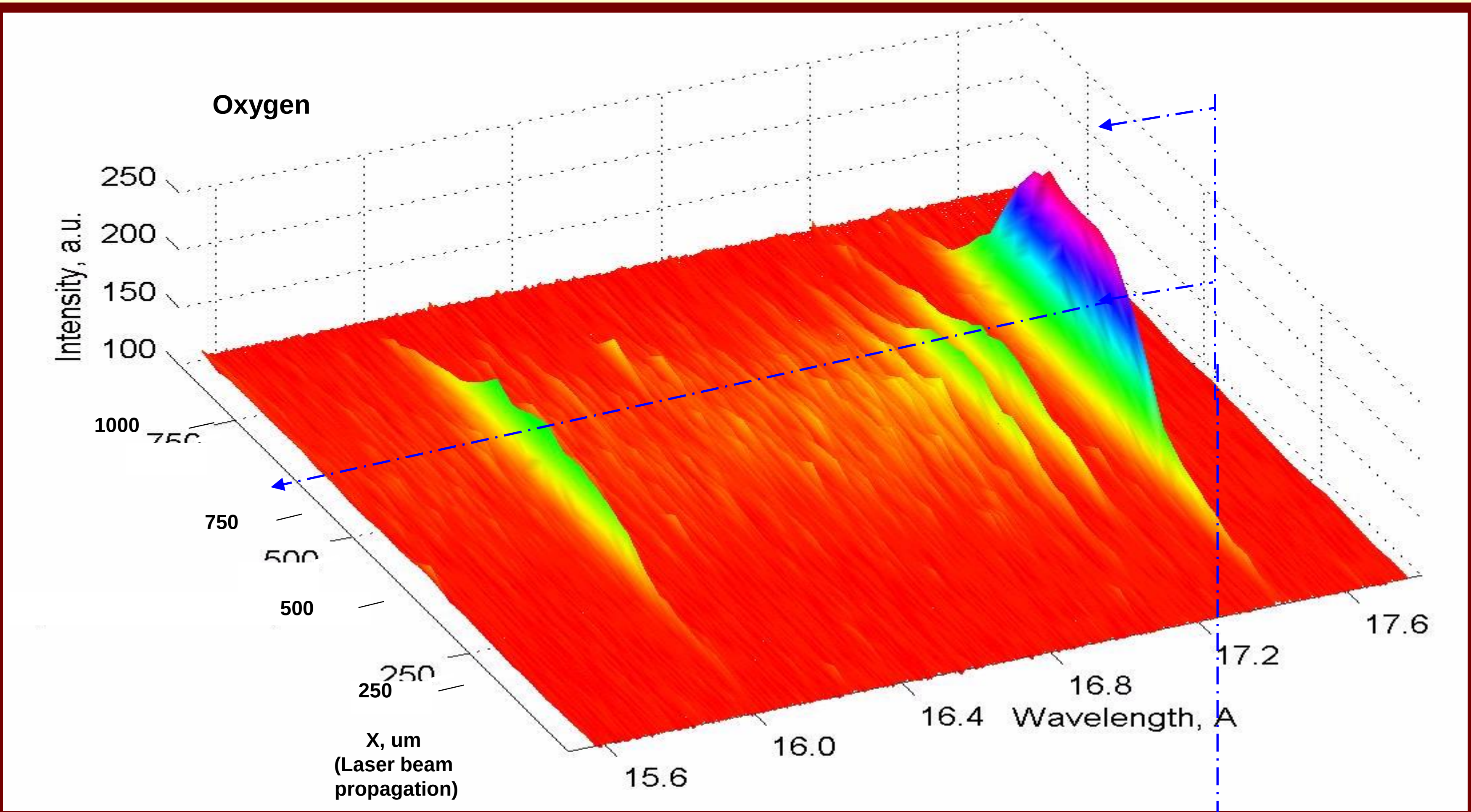

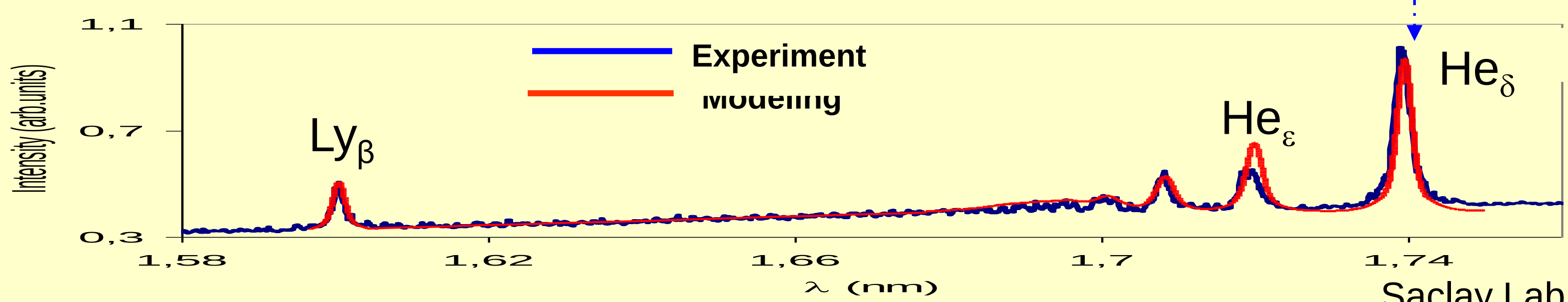

Saclay Lab., France

High spectral resolution is a crucial point for plasma diagnostic

Simulation

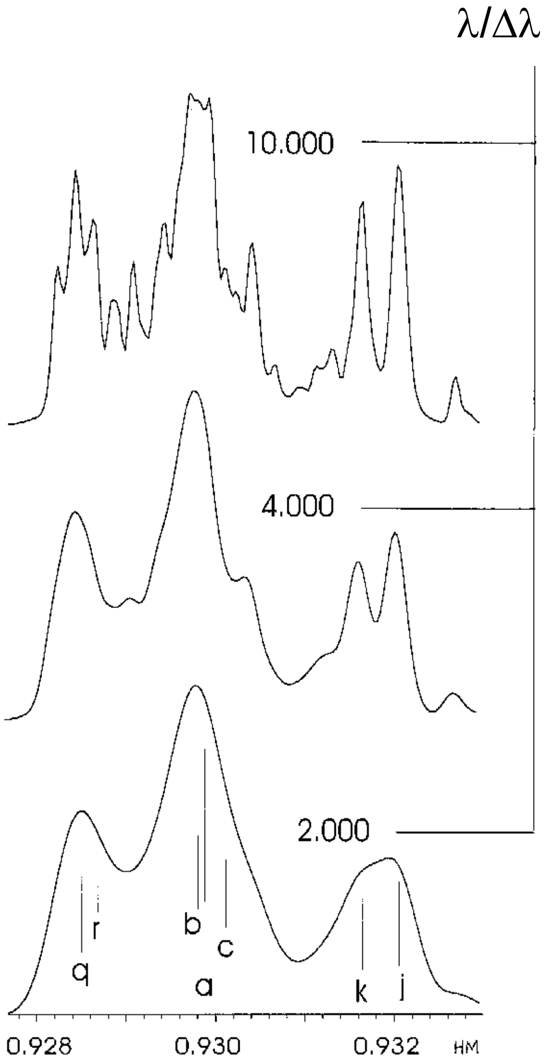

Experiment

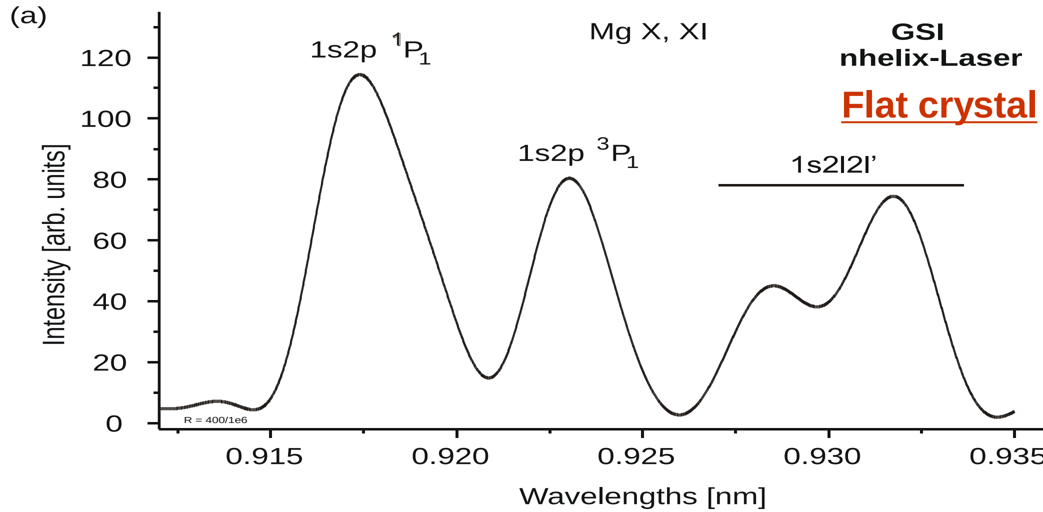

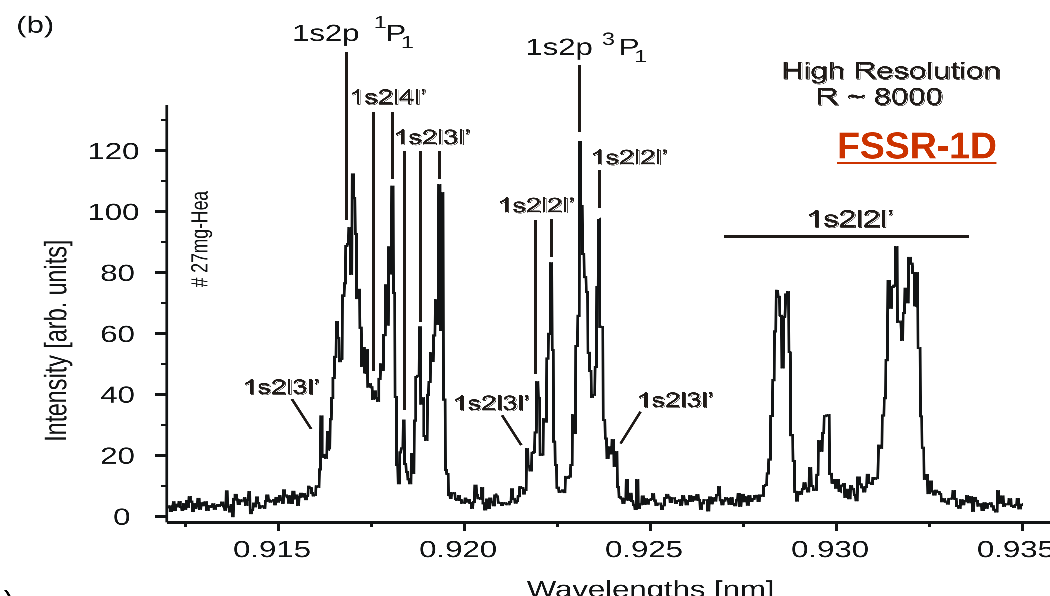

Ref.: F.B.Rosmej et al. PRA, **63**,n6,063409 (2001);

High spatial resolution gives very important information about radiation properties of plasma from different zones of laser interaction with matter

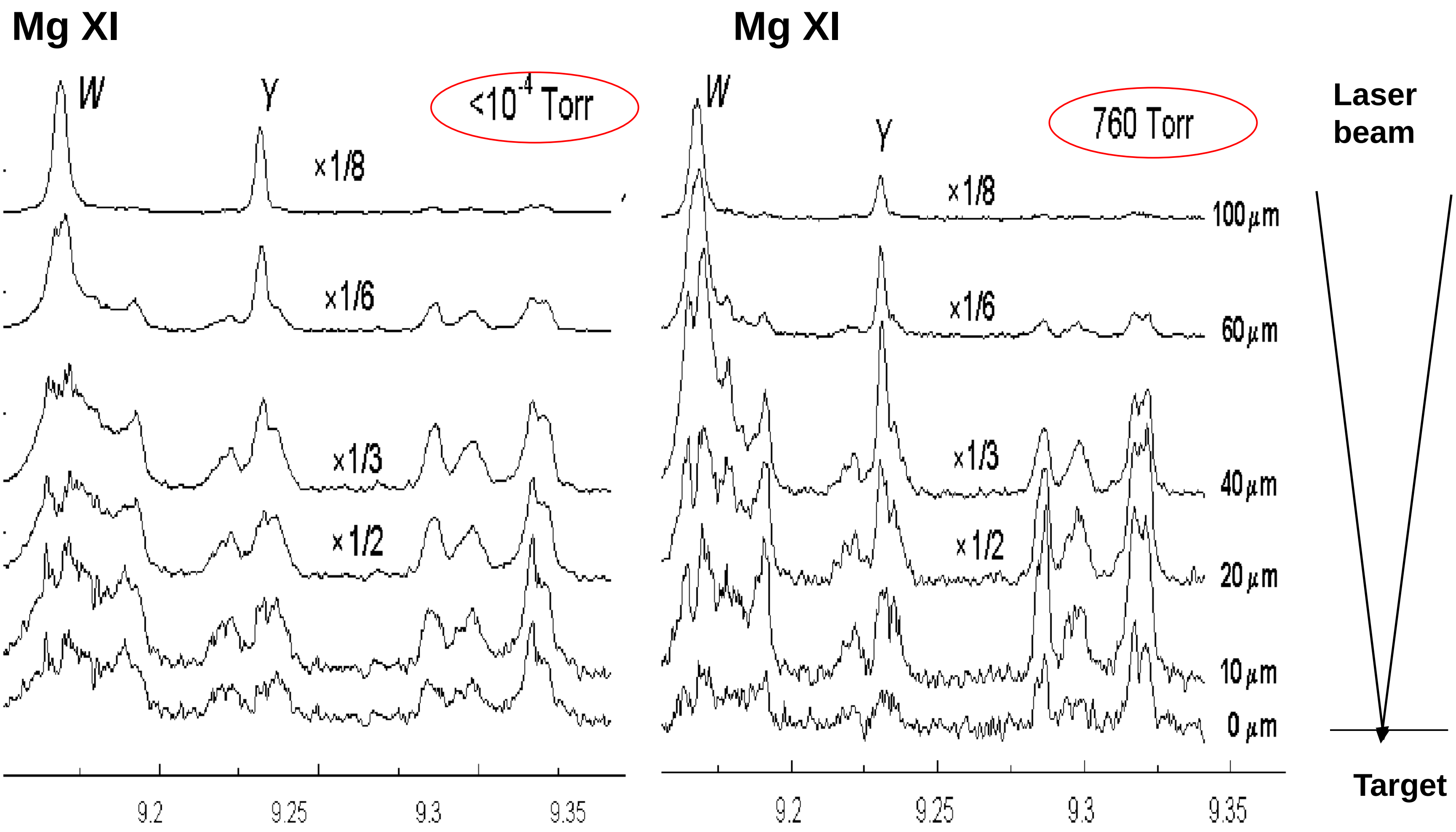

XeCl laser (λ = 0.308 μm, τ = 10 ns, E =1.3 J)
ENEA, Frascati, Italy

High spatial resolution allows to resolve near by plasma objects and measure their spectra with high spectral resolution

VNIIFTRI

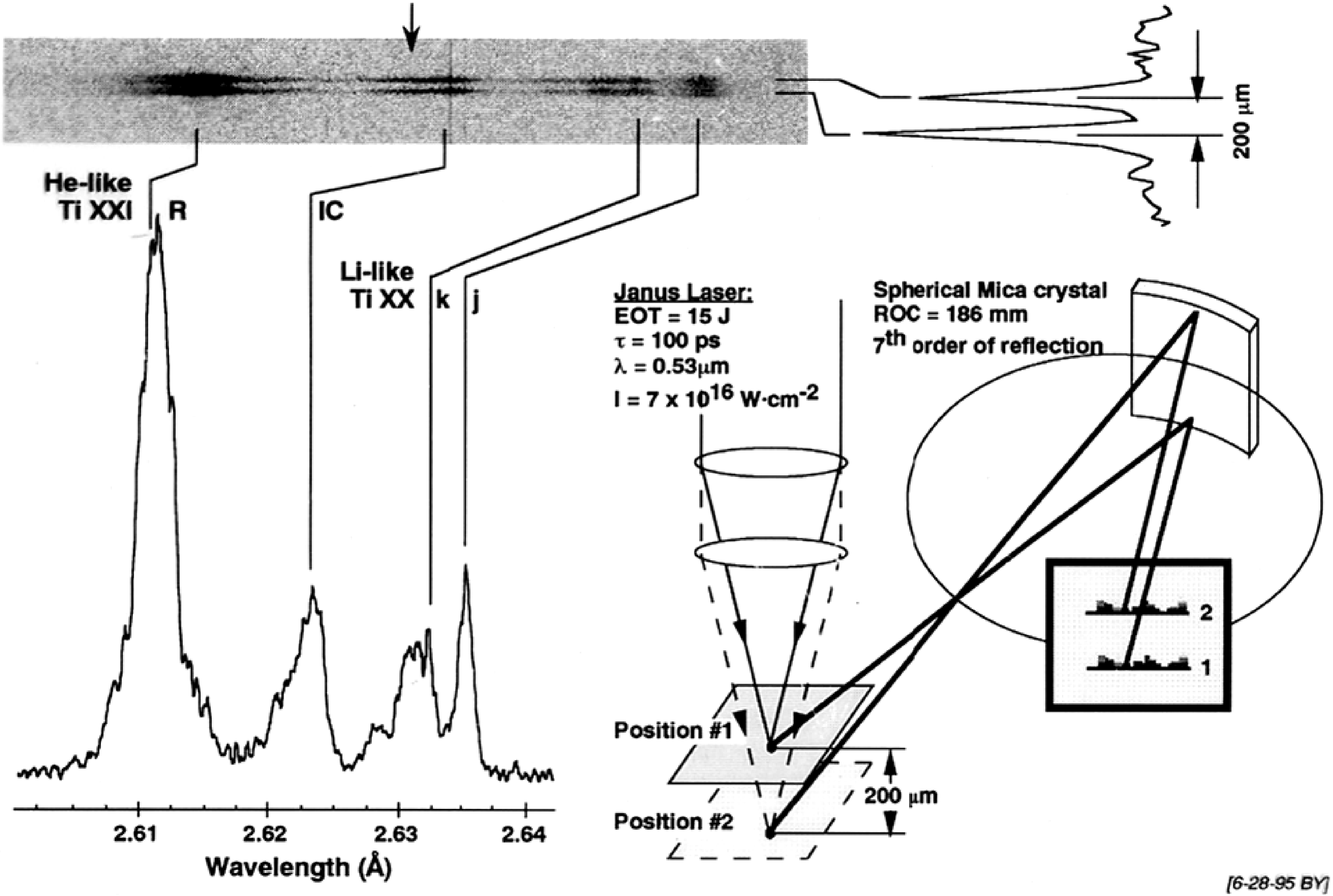

Radiation properties of elongated plasma objects could be measured

Diagnostics of the X- ray laser media parameters, using FSSR spectrometer

Ne-like Fe (λ = 25.5 nm) transient collisional x-ray laser

Ne-like Cr (λ = 28.5 nm) transient transient collisional x-ray laser (Injector + amplifier scheme)

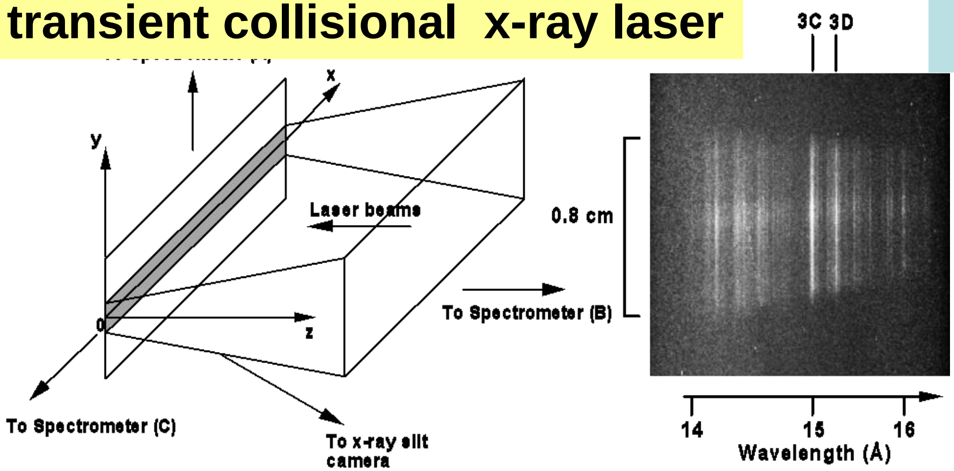

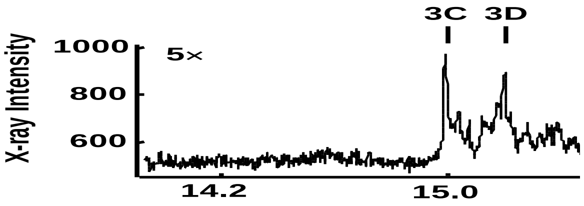

ns-pulse

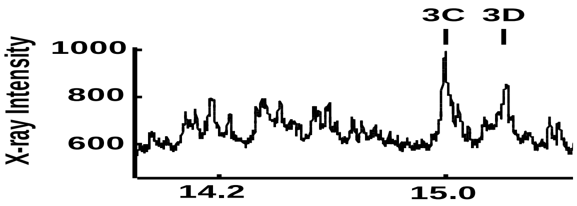

ns+ps-pulse

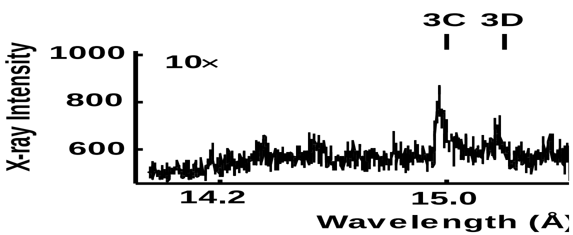

ps-pulse

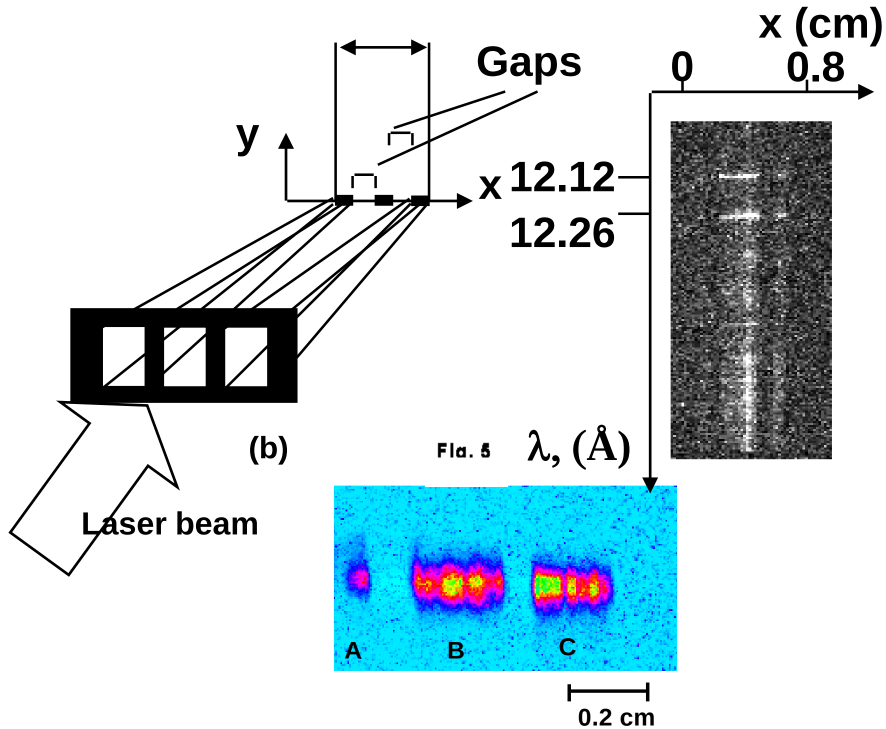

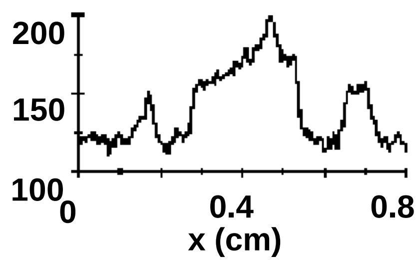

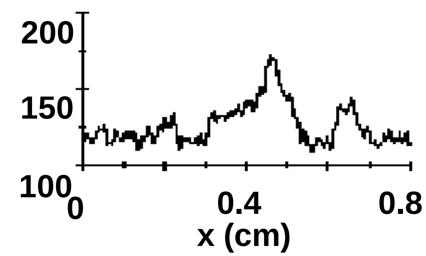

COMET facility (LLNL, USA)

Applications for high precision measurements of wavelengths

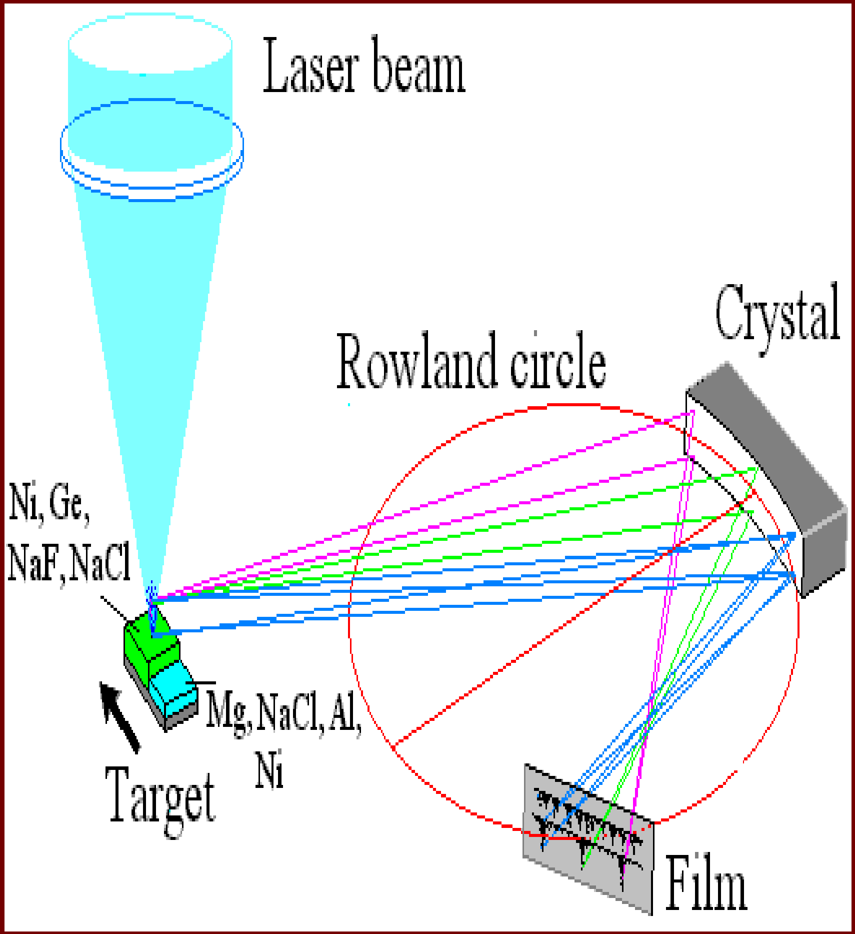

Nd:glass laser (λ = 1.06 μm, τ = 2 ns, E =25 J)
MISDC of VNIIFTRI, Russia

FSSR-1D; Mica, R=150 mm

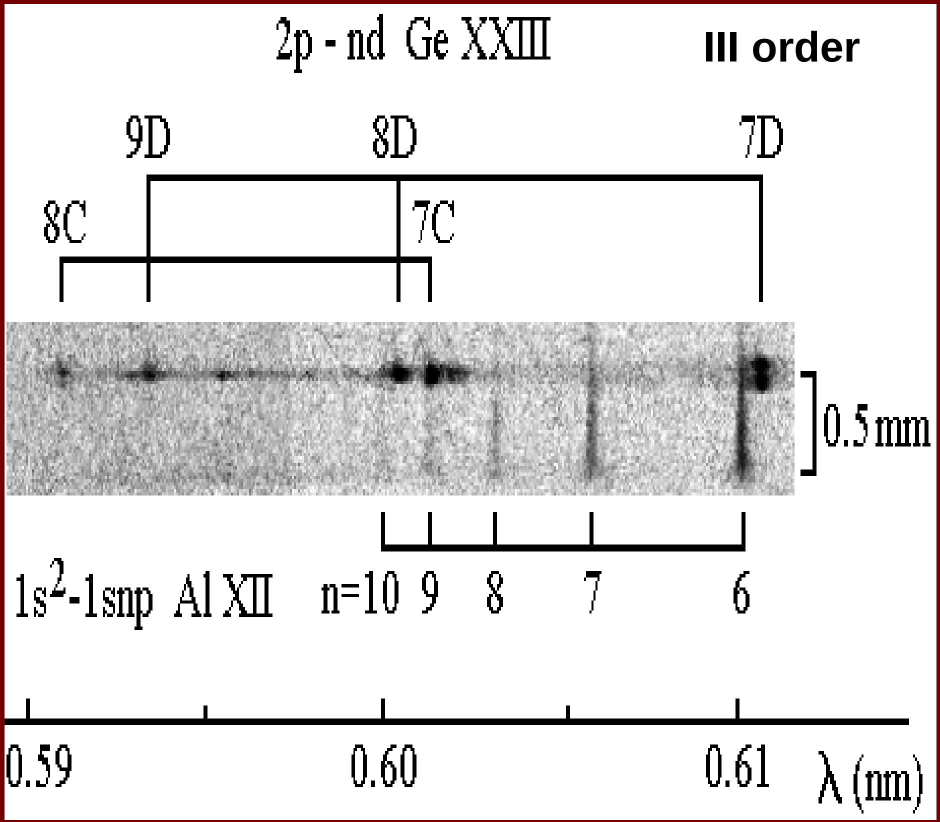

A.L.Osterheld et al. PRA, 54, 3971-3976 (1996)

Diagnostics the homogenity of plasma production.

Femtosecond laser interaction with clusters:

No clusters near the axis of Laval nozzle- no X-ray emission

FSSR-1D (1)

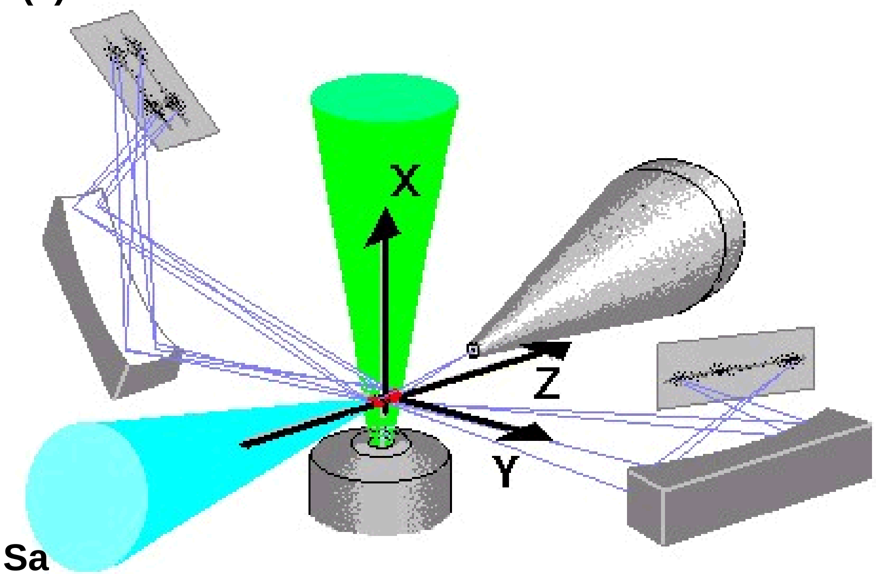

45 fs, 15 mJ, Ti:Sa Laser beam

I order of reflection

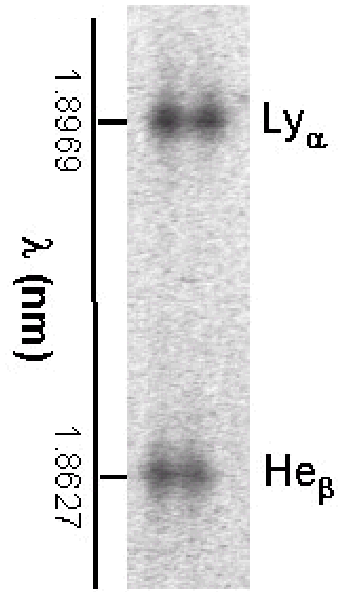

FSSR-1D (1)

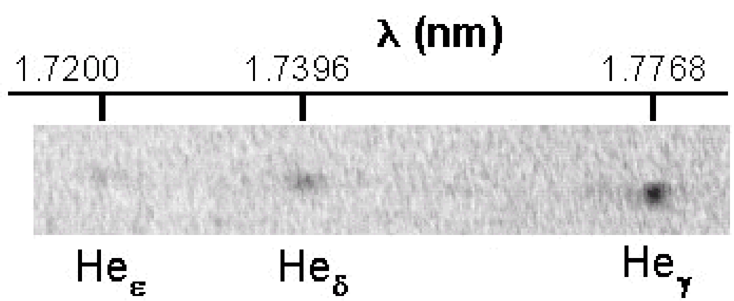

FSSR-1D (2)

I order of reflection

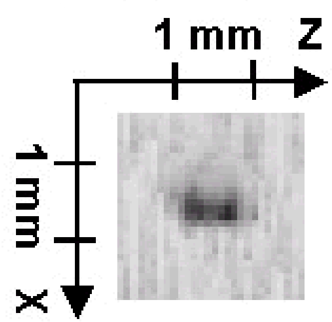

CO_2 clusters

CELIA, Bordeaux University, France, 2000

Diagnostics the homogenity of plasma production.

Femtosecond laser interaction with clusters:

Conical nozzle create homogenous cluster jet near the axis

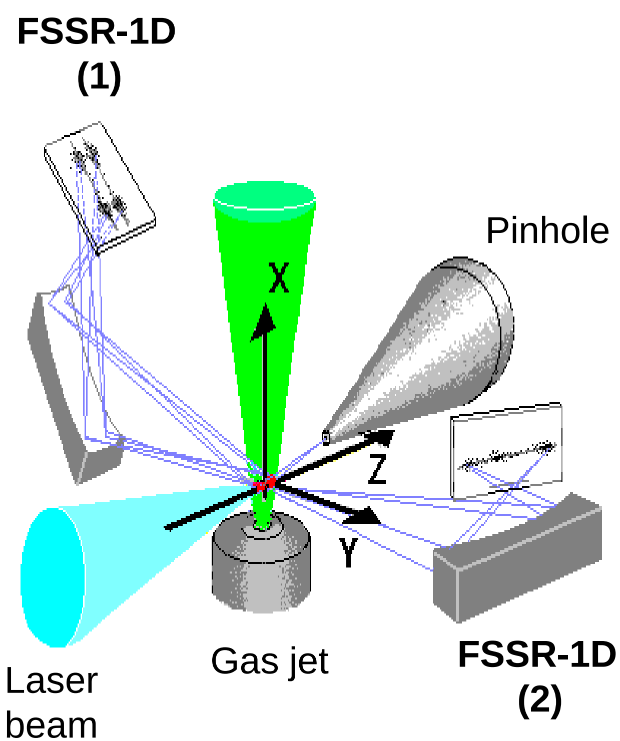

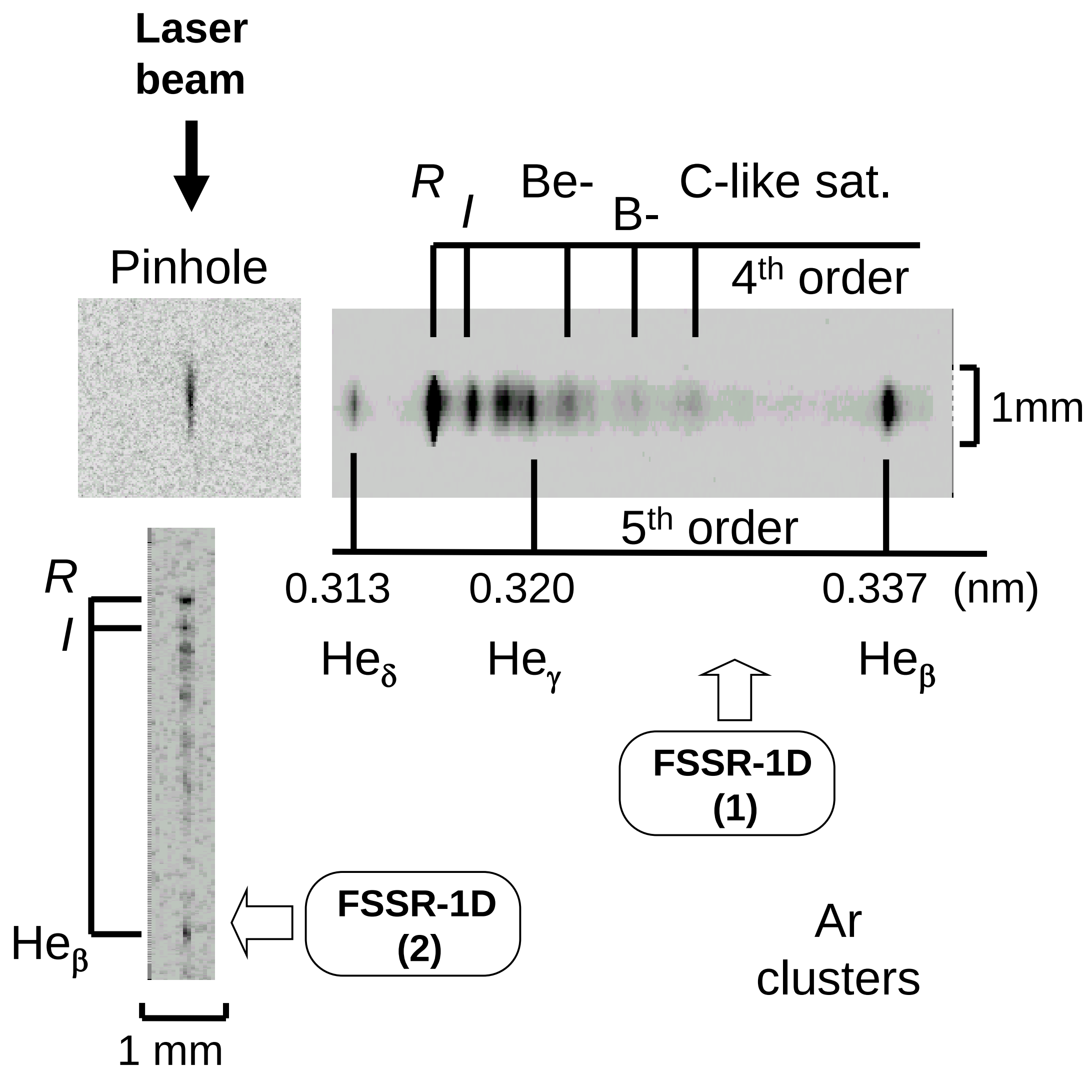

Conical nozzle

No realignment for another spectral range!

CELIA, Bordeaux University, France, 2000

Diagnostics the homogenity of plasma production.

Femtosecond laser interaction with CO_2 clusters:

Strong influence of fs laser contrast to the radiation properties of produced plasma

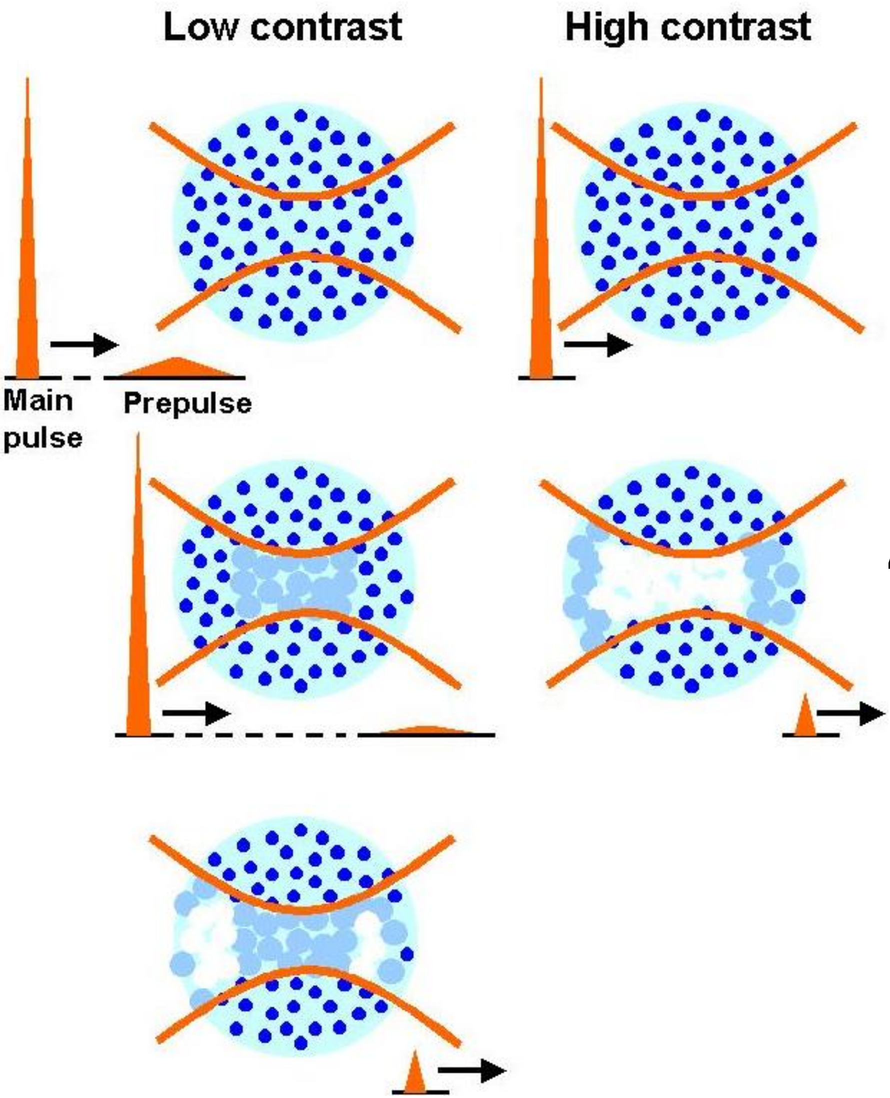

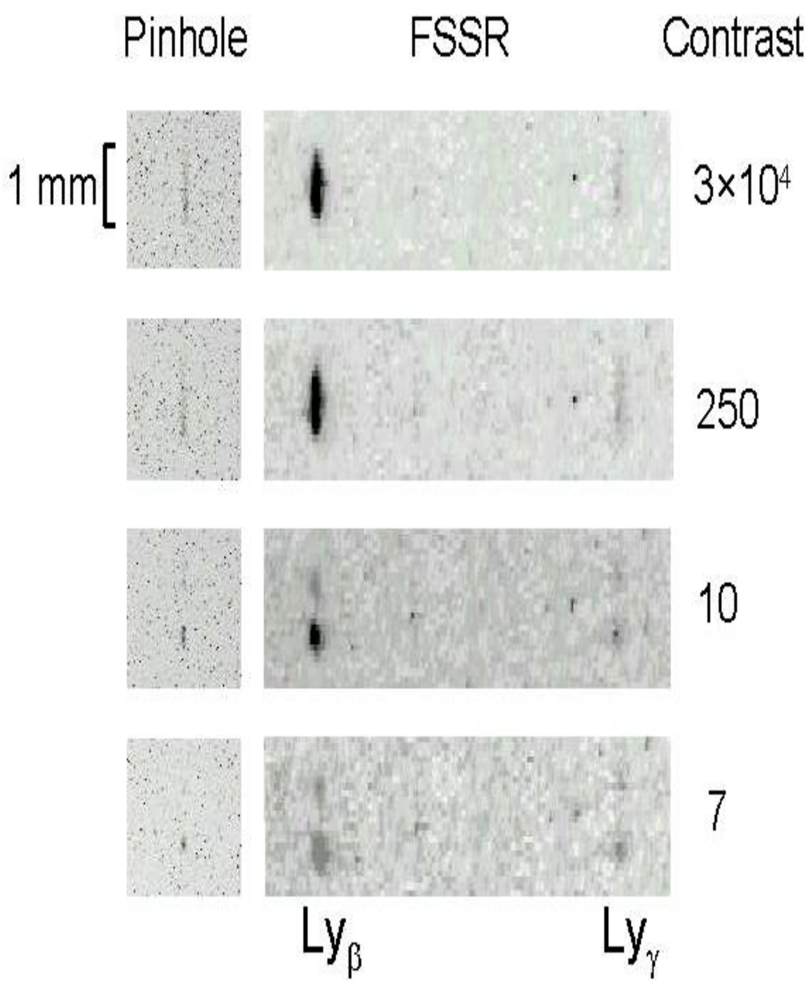

CELIA, Bordeaux University, France

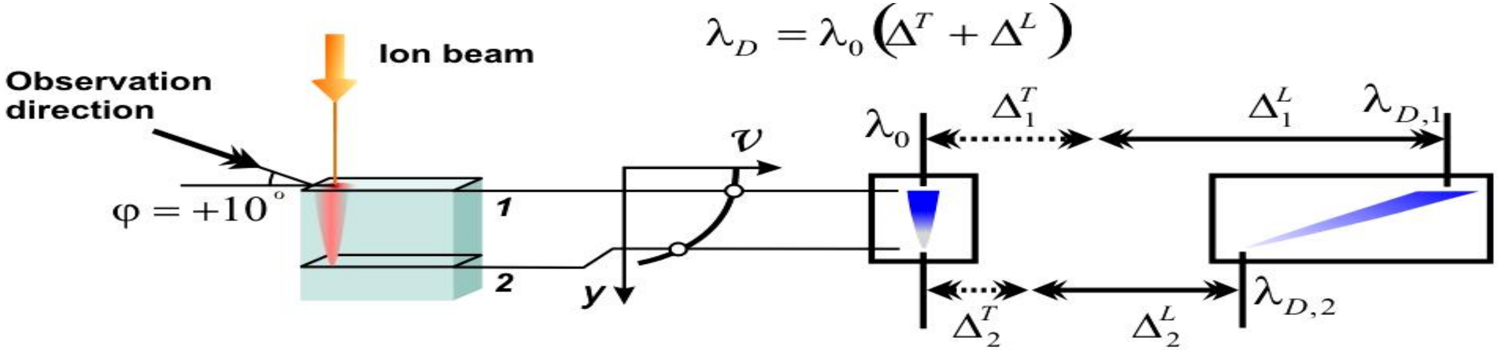

Projectile ion spectra

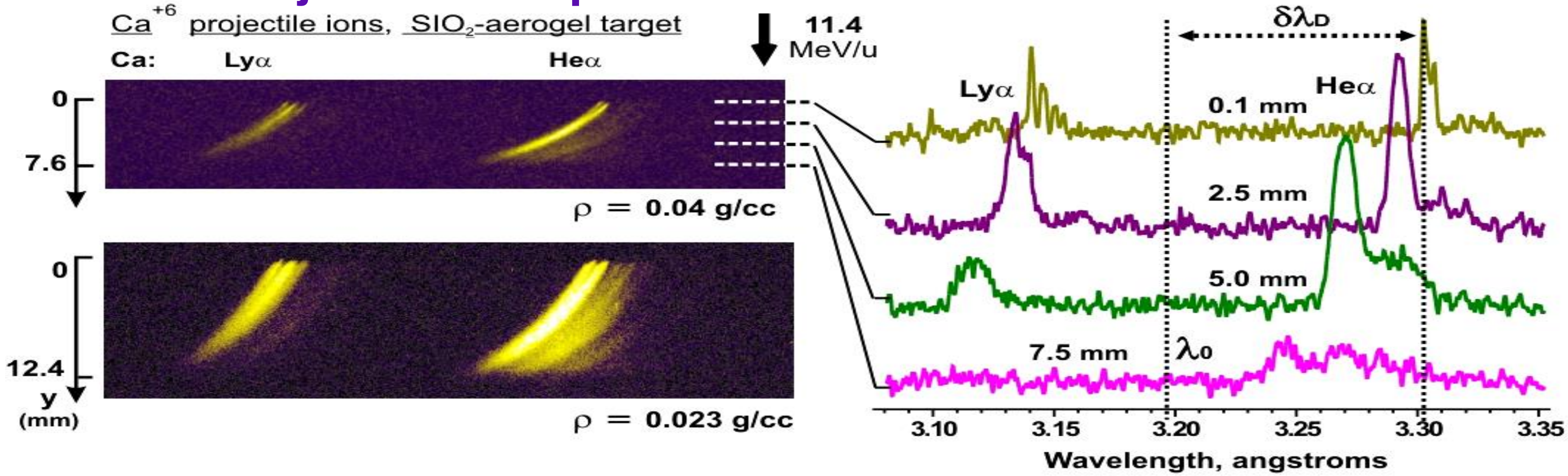

Excitation evolution of target along the projectile ion track

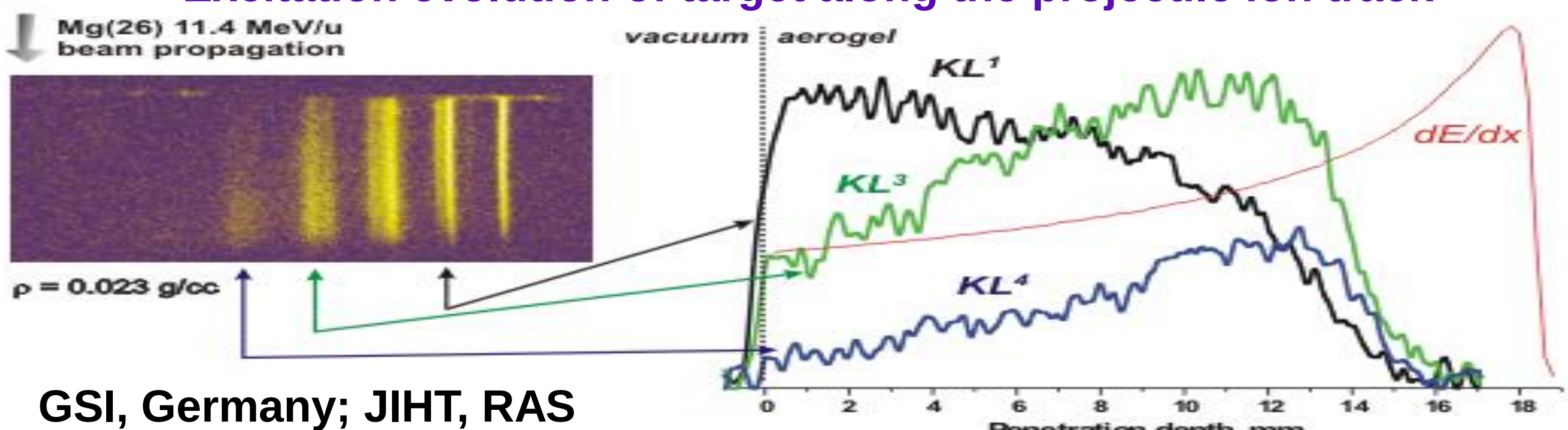

GSI, Germany; JIHT, RAS

Focusing spectrometer with spatial resolution (FSSR)

(No slit to obtain spatial resolution!)

FSSR-2D

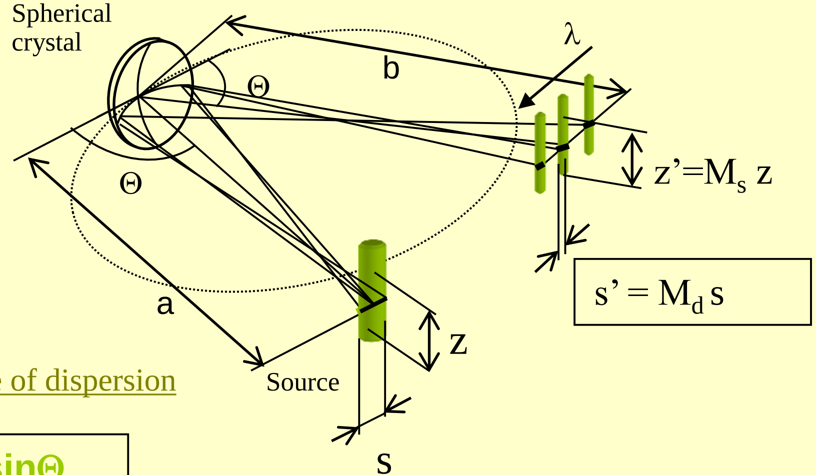

Plane of dispersion

1/a + 1/b =2/RsinΘ

a = Rb / (2bsinΘ - R)

b = M_s a

$$\mathbf{M_d} = \frac{R\left[a - \cos\Theta\left(2a\cos\Theta - R\right)\right]}{\left(R\cos\Theta - a\right)\left(2a - \cos\Theta - R\right)}$$

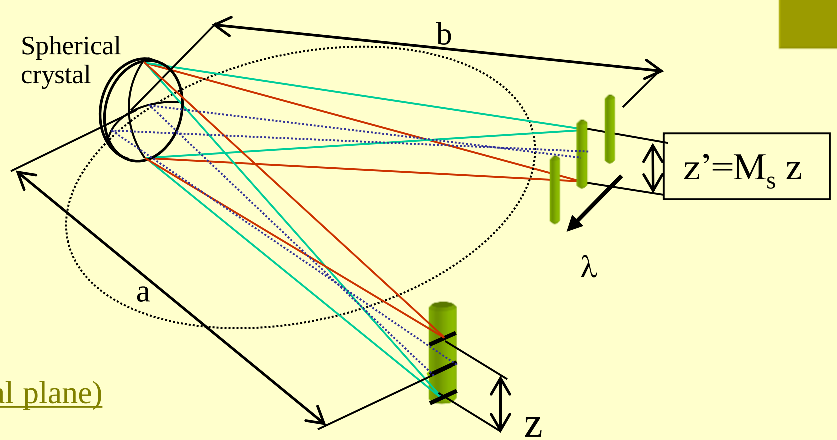

(Sagittal plane)

Ref.: A.Faenov et al., Physica Scripta, **50**, 333-338 (1994); I.Skobelev et al., JETP, **81** , 692-717 (1995); T.Pikuz et al., J.X-ray Science and Technology, **5**, 517-521 (1995)

Two dimensional spatial resolution gives a very important information about radiation properties of different ions inside the plasma expansion plume (the angle distribution of ions acceleration could be measured)

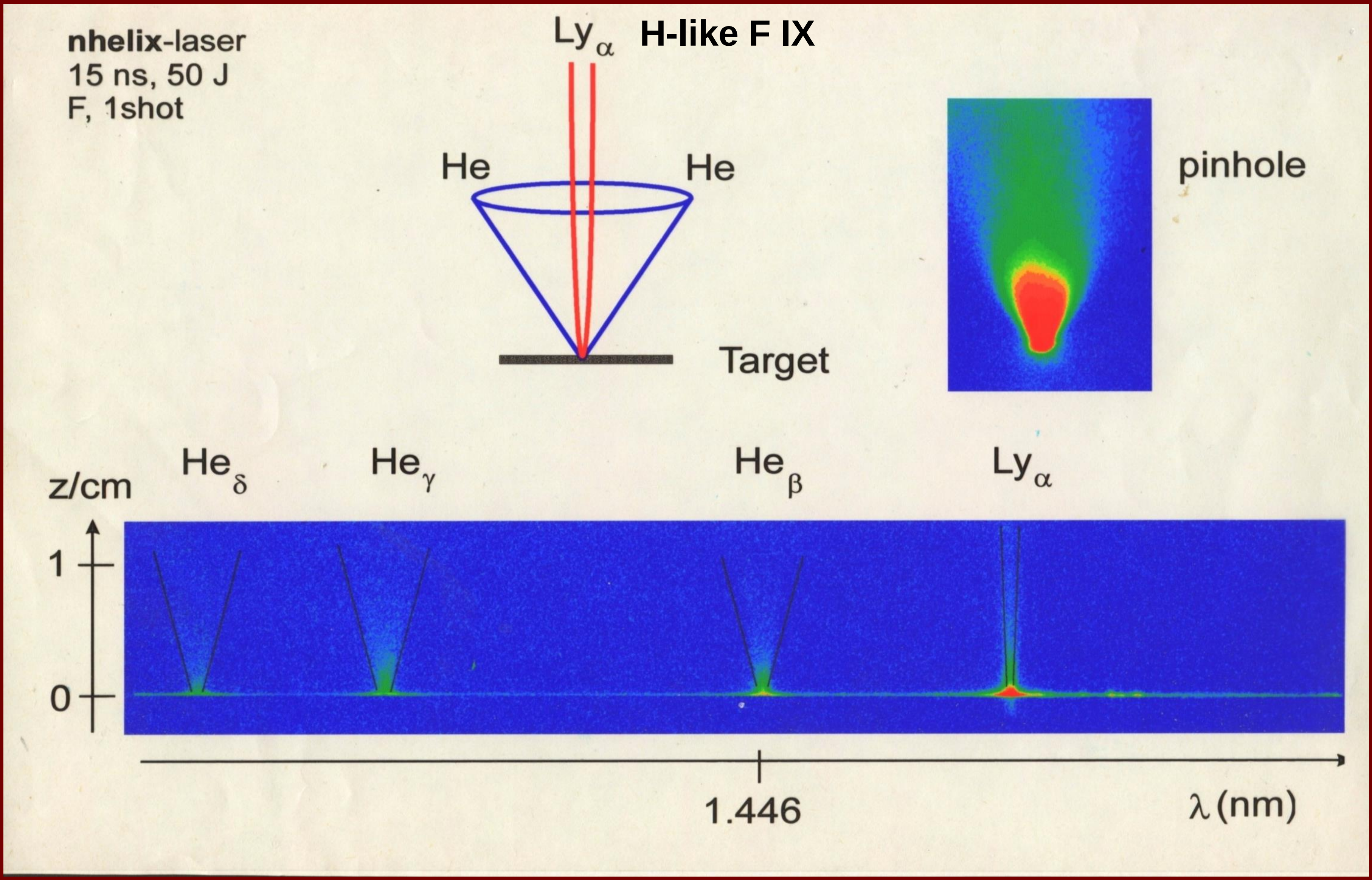

Observation of magnetic field influence on the laser produced plasma expansion (Astrophysical applications)

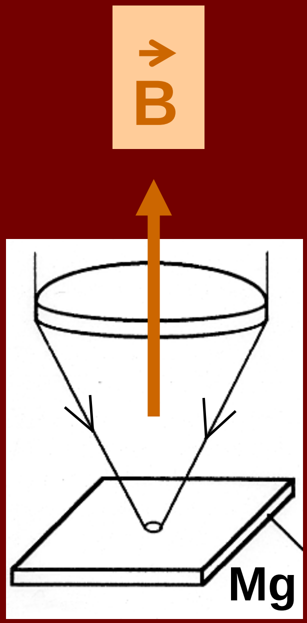

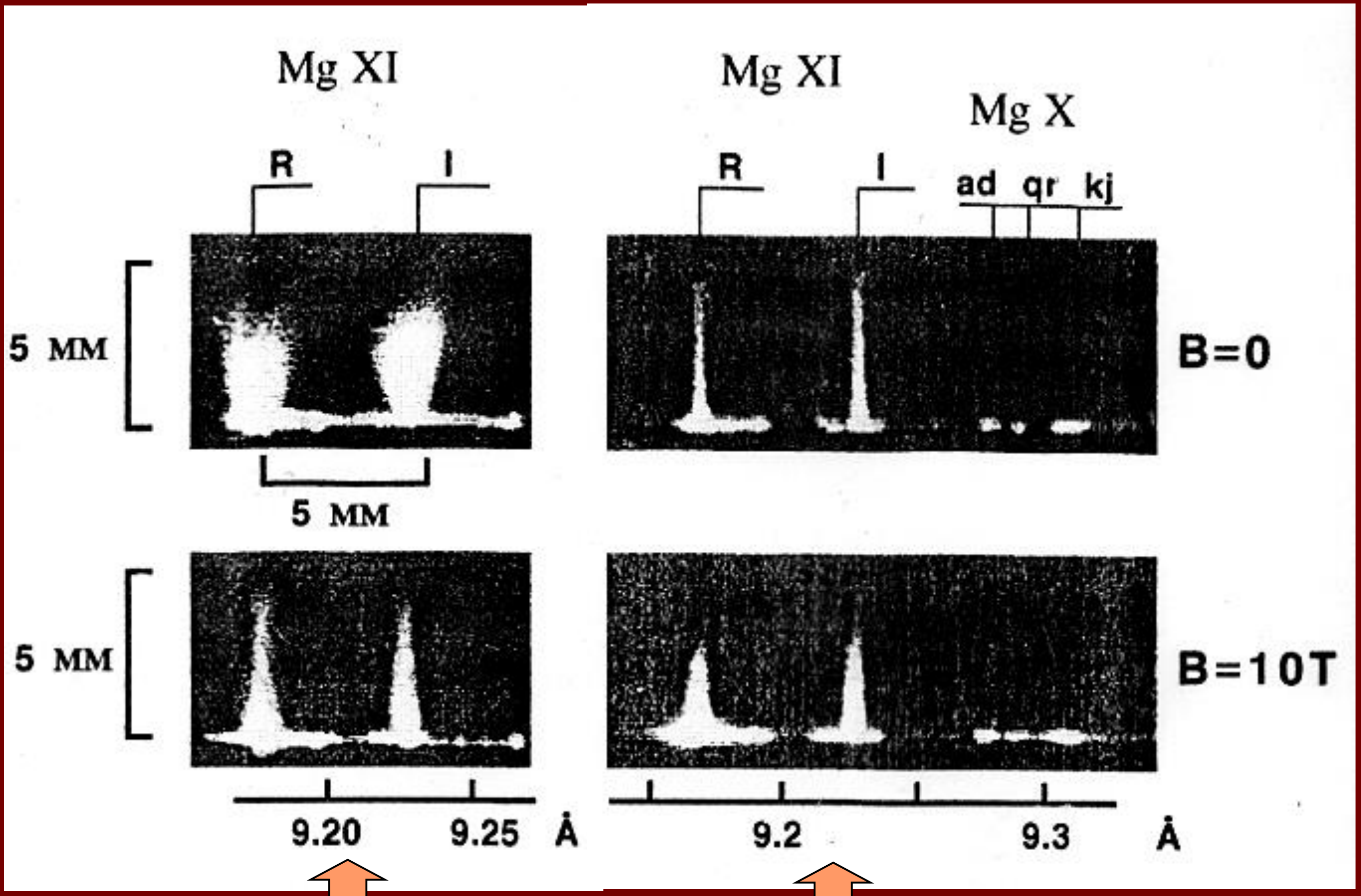

FSSR-2D

FSSR-1D

IFPILM, Warsaw, Poland

Observation of radiation properties of laser produced plasma under interaction with solid obstacles (Astrophysical applications)

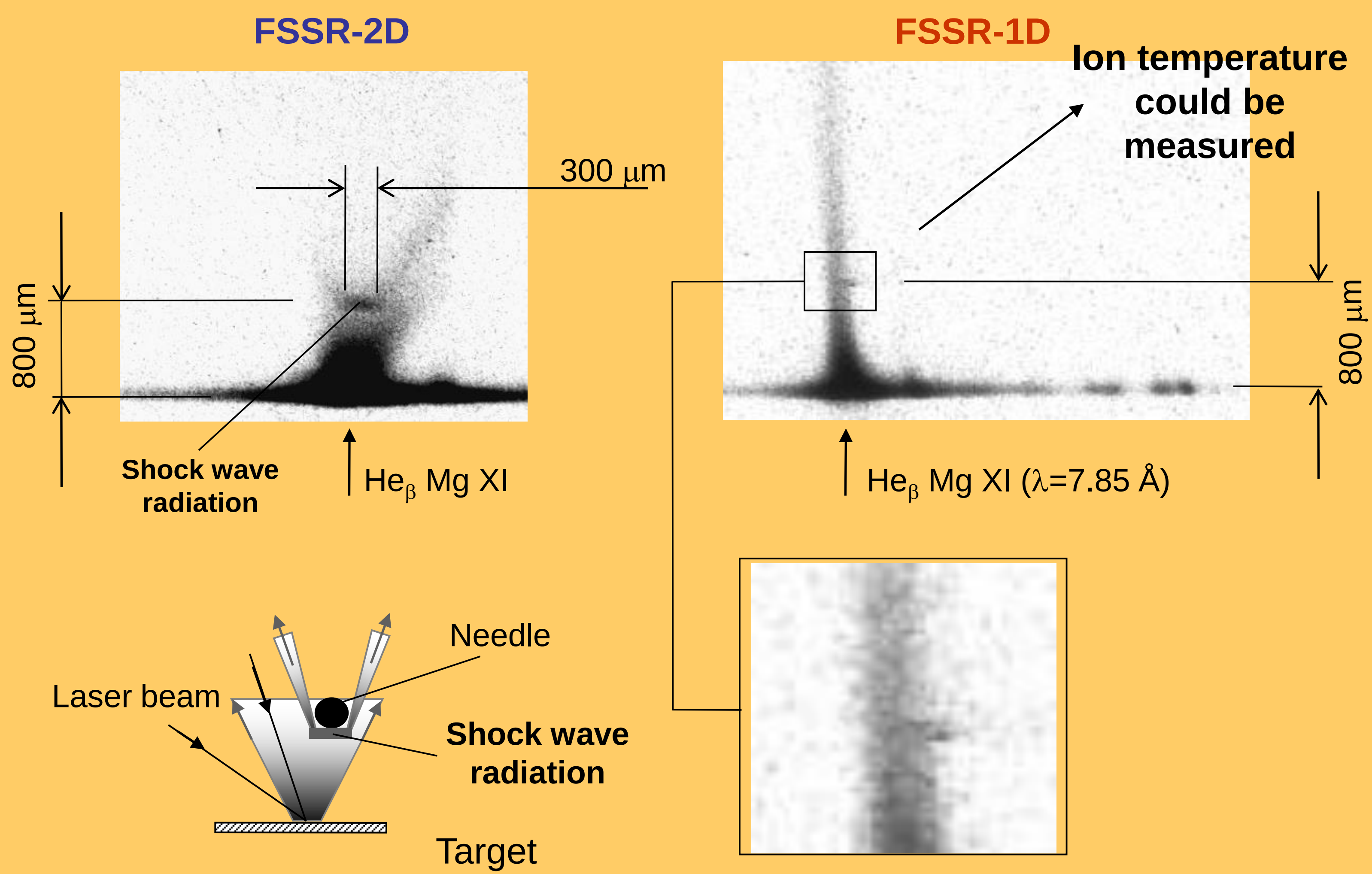

Ng:glass laser (λ = 1.06 μm, τ = 15 ns, E =5 J)

Tor Vergata University, Rome, Italy

X-ray monochromatic backlighting scheme

(is widely used now in many Labs for investigation different plasma objects)

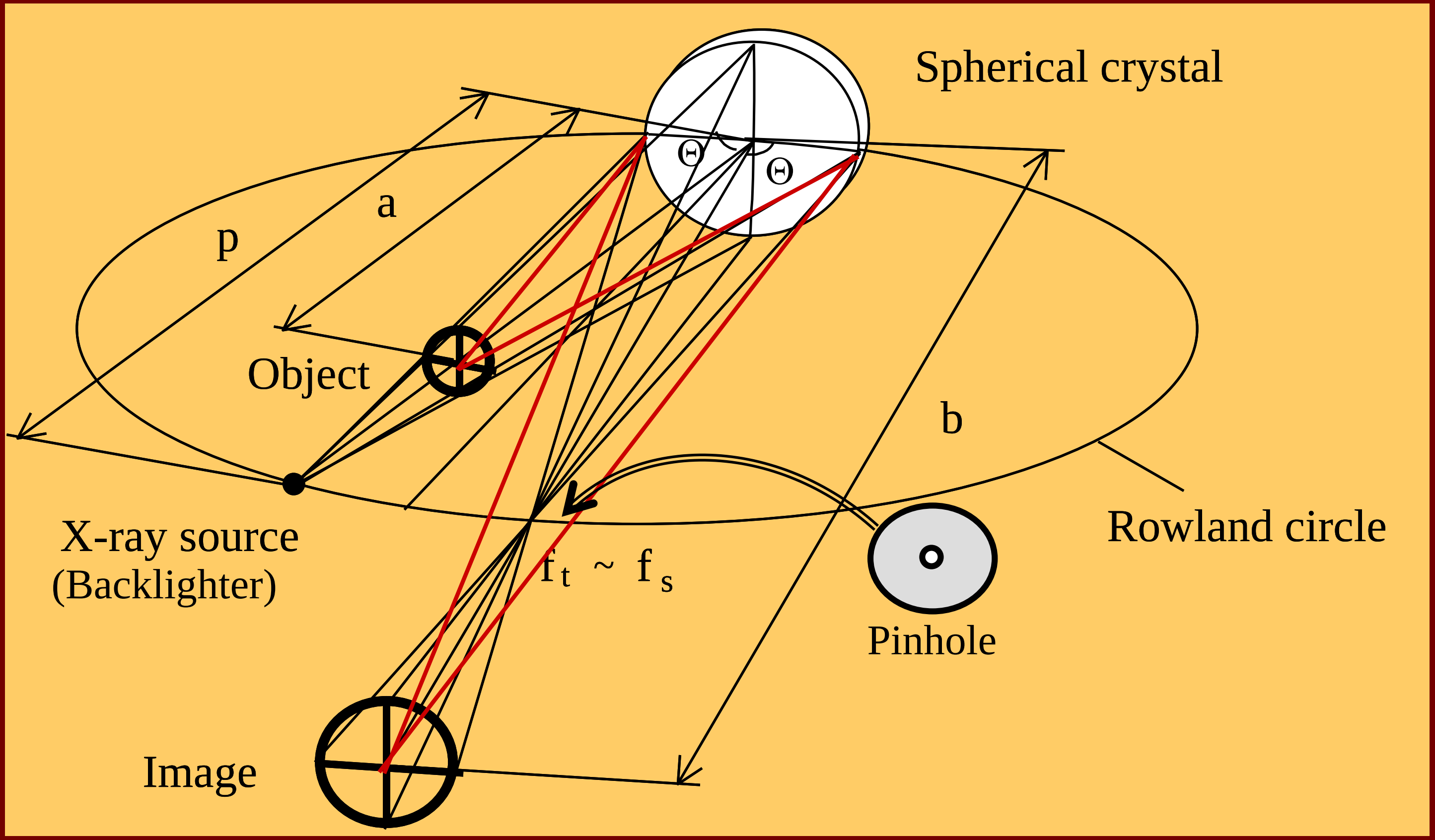

$$1/a + 1/b = 2\sin\theta / R$$

$$M = b / a$$

Bragg angles: $85^{o} \div < 90^{o}$ deg

The Test Images of a 1500 lpi Mesh demonstrated a very high spatial resolution in a big field of view

NRL

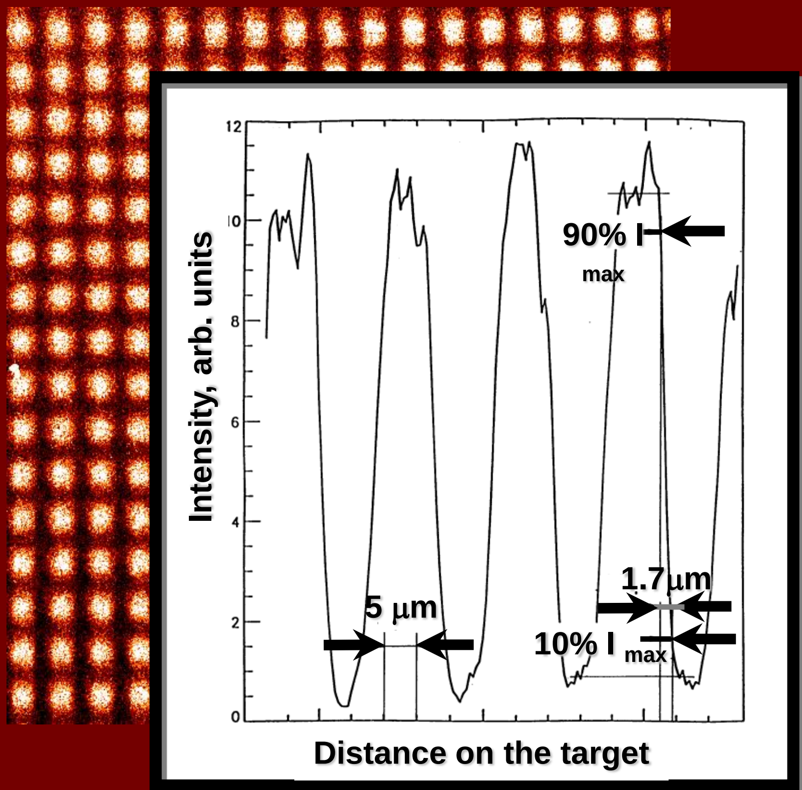

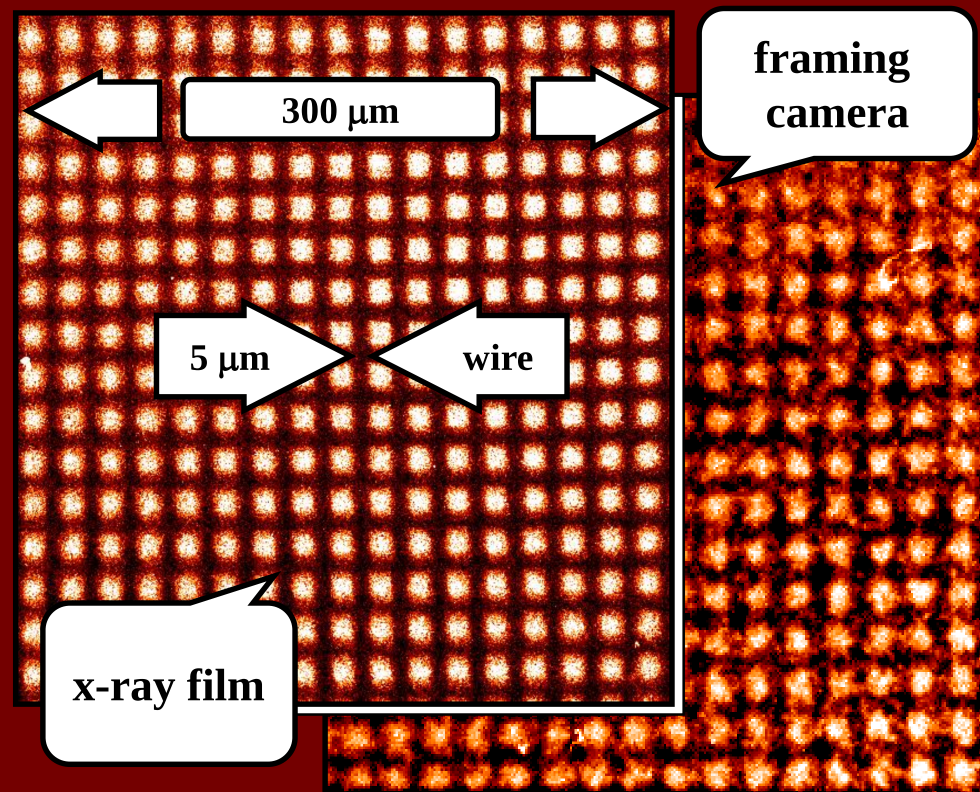

The resolution of the x-ray optical system reaches 2 μm

Due to the noise of the framing camera, time resolved images have worse but still very good resolution of 3.5 - 5 μm.

Y. Aglitskiy et al.

General Scheme of the Backlighting Experiment on the NRL NIKE Laser

NRL

The main target is turned in order to be in more favorable position for imaging. Two images are delivered to the assigned vacuum port about 2000 mm away from the target with the accuracy of 2 arcmin.

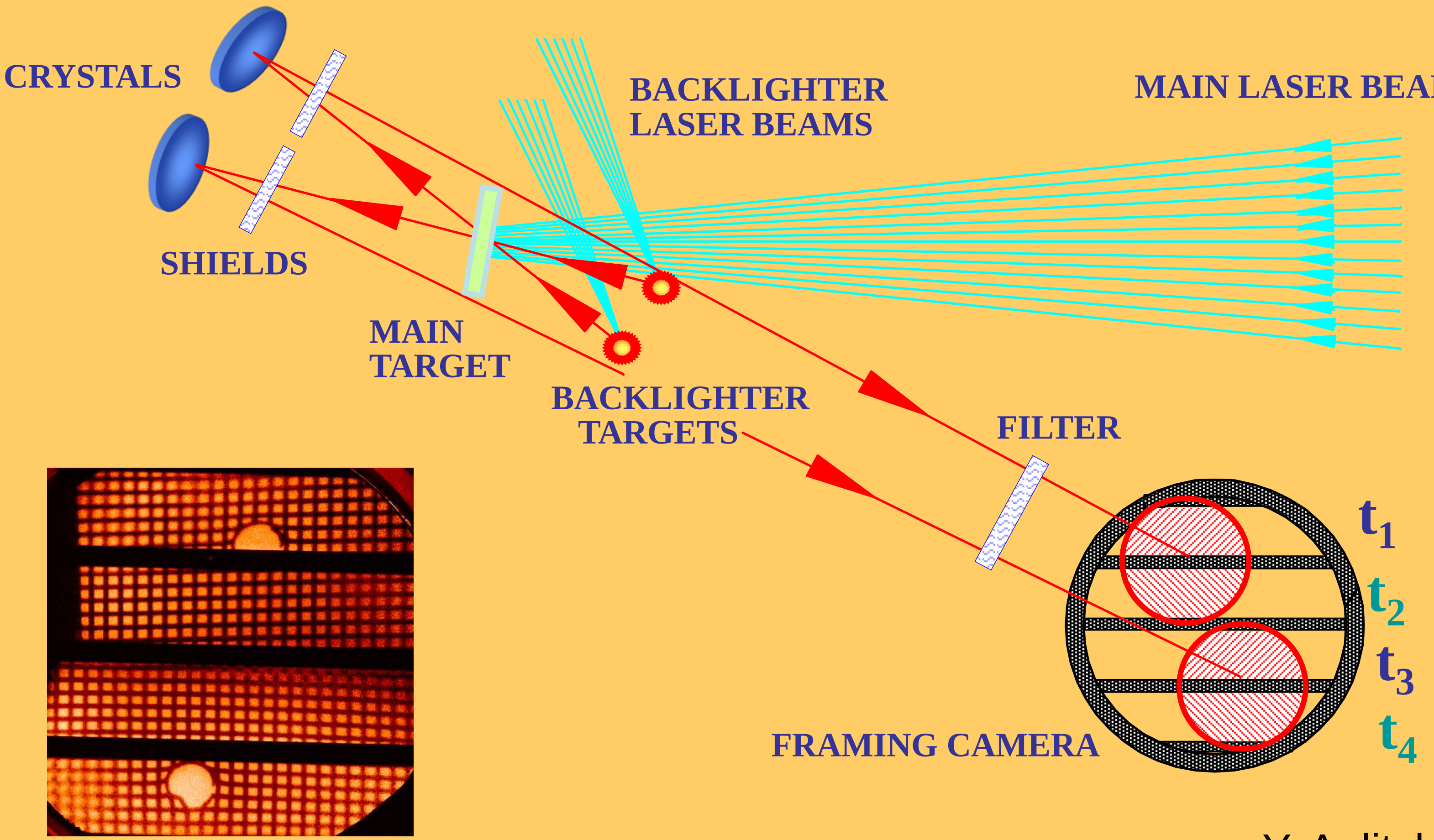

Y. Aglitskiy et al.

Improved Sensitivity in Rayleigh-Taylor Diagnostics

An experiment was performed with 40 mm thick plastic targets with sinusoidal modulation of initial amplitude of 0.45 mm peak-to-valley.

NRL

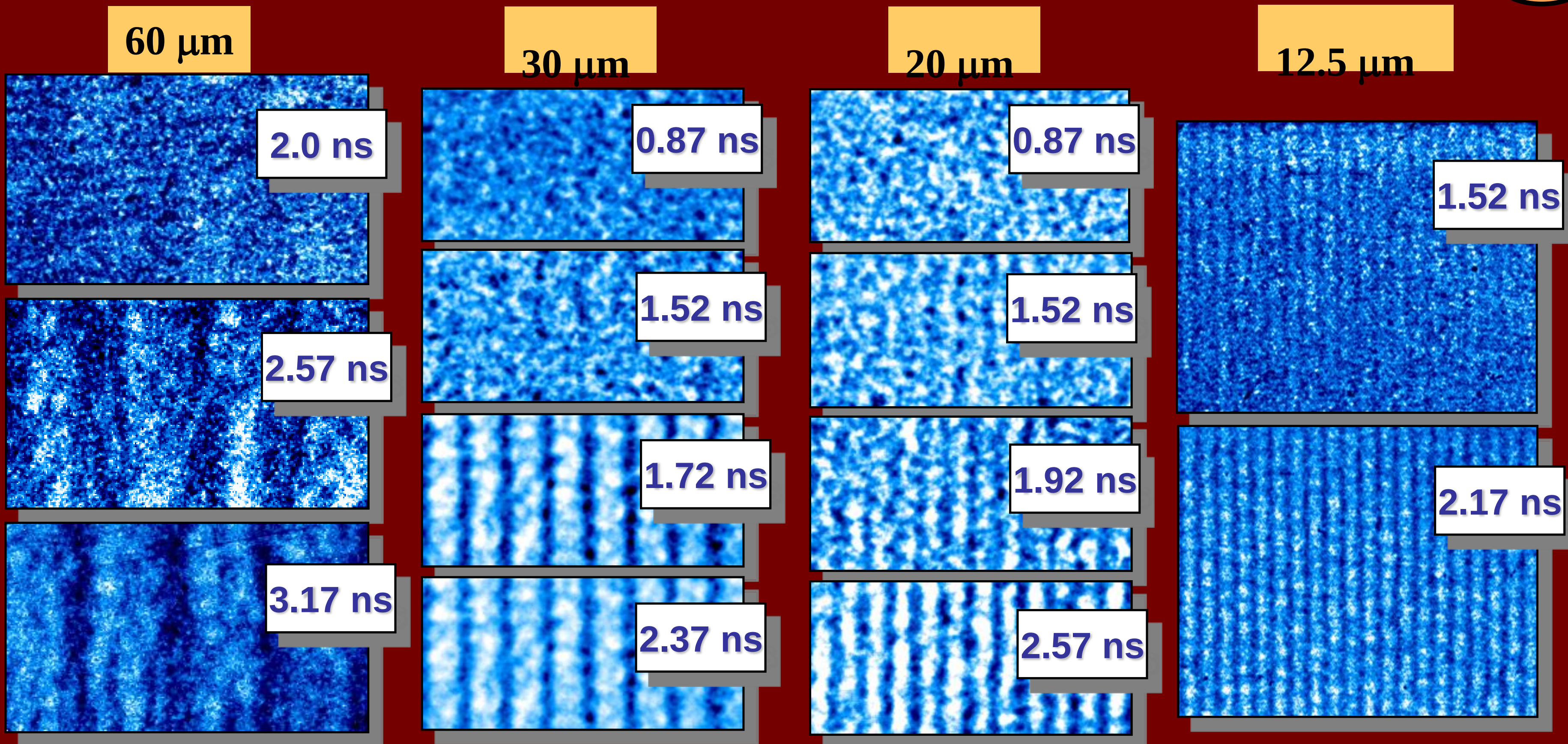

The use soft 1.47 keV x-rays used allows smal amplitude perturbations to be observed. The frames are 200 ps exposures.

Y. Aglitskiy et al.

Test experiments show very high quality of spherically bent crystals in X-ray

The 1.865 keV system was tested on the Z-Beamlet calibration chamber

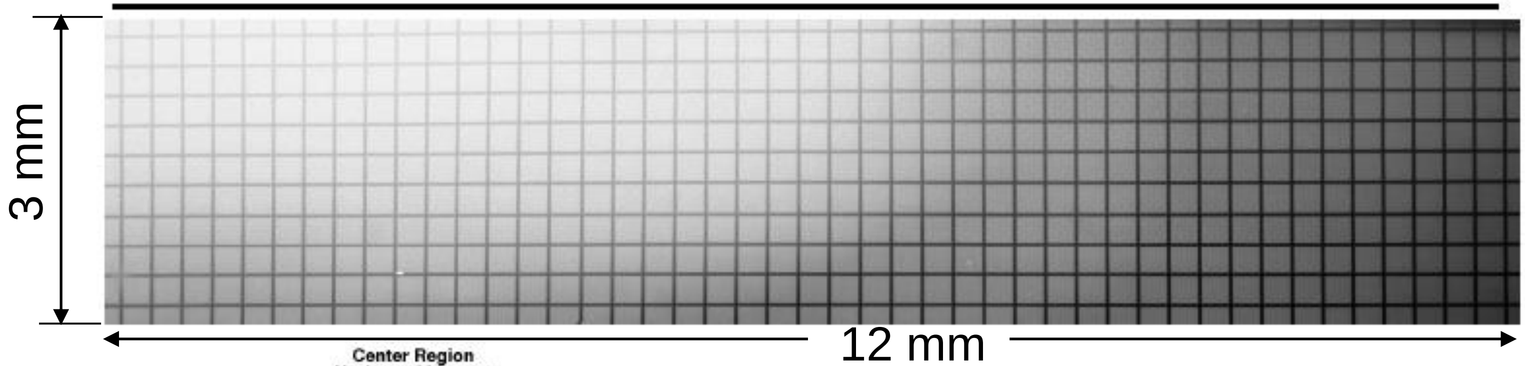

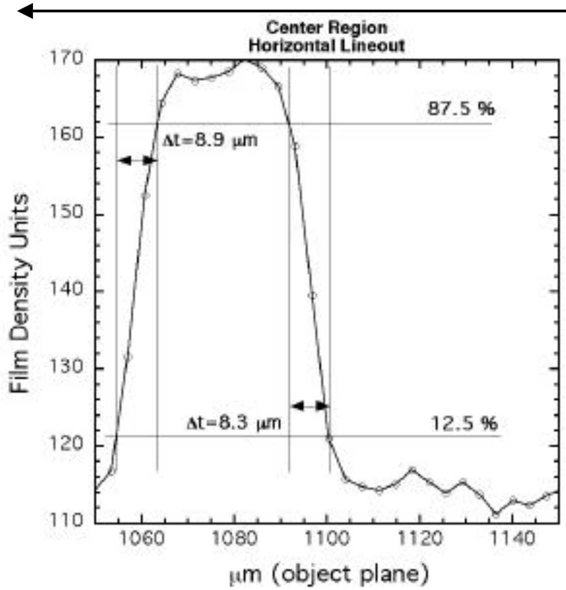

- The Si He-α imaging system has been tested in the ZBL calibration chamber in a Z-identical geometry.
- Images of 33.5 μm diameter electroformed meshes have been obtained with ~10 μm resolution.

D.B. Sinars et al.

Sandia National Laboratories

1.865 keV monochromatic backlighting image of a 20mm, 300 (7.41 μm) W wire array

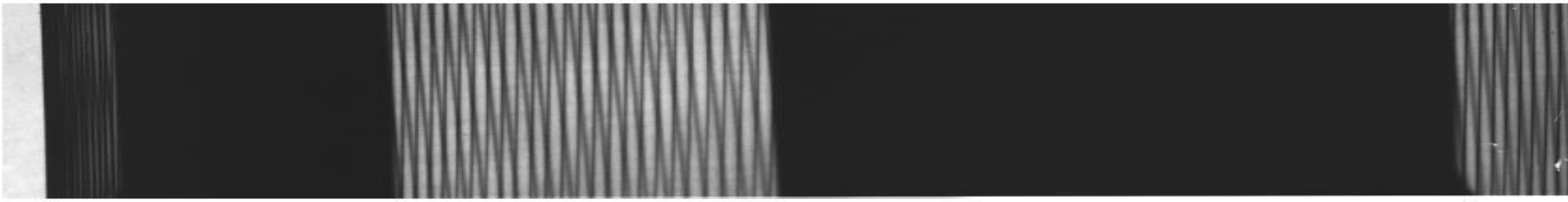

Edge of wire array (r=10 mm)

r= 6 mm

r= 2 mm

r= -6 mm

Time is approximately 33% of implosion time

Wire array edge shows small bumps (~15 by 30 μm)

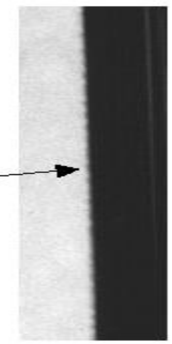

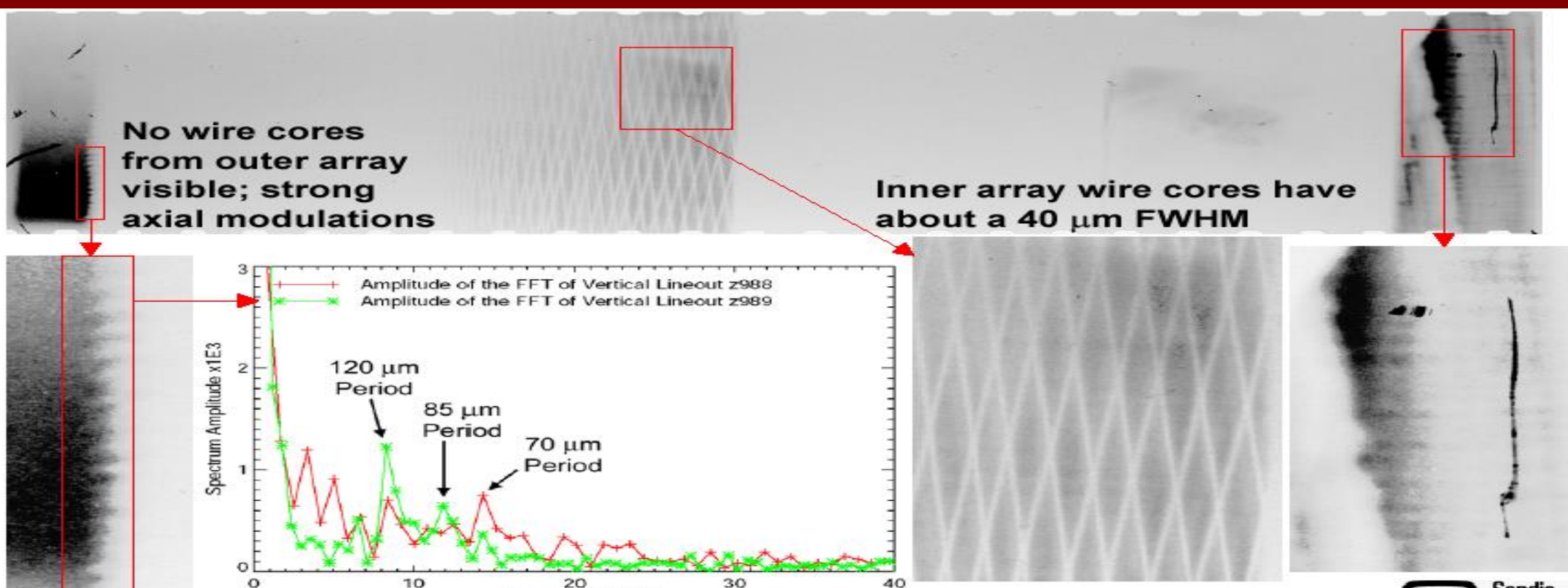

D.B. Sinars et al.

Experimental result on wire-array Z pinch (Z-beamlet facility)

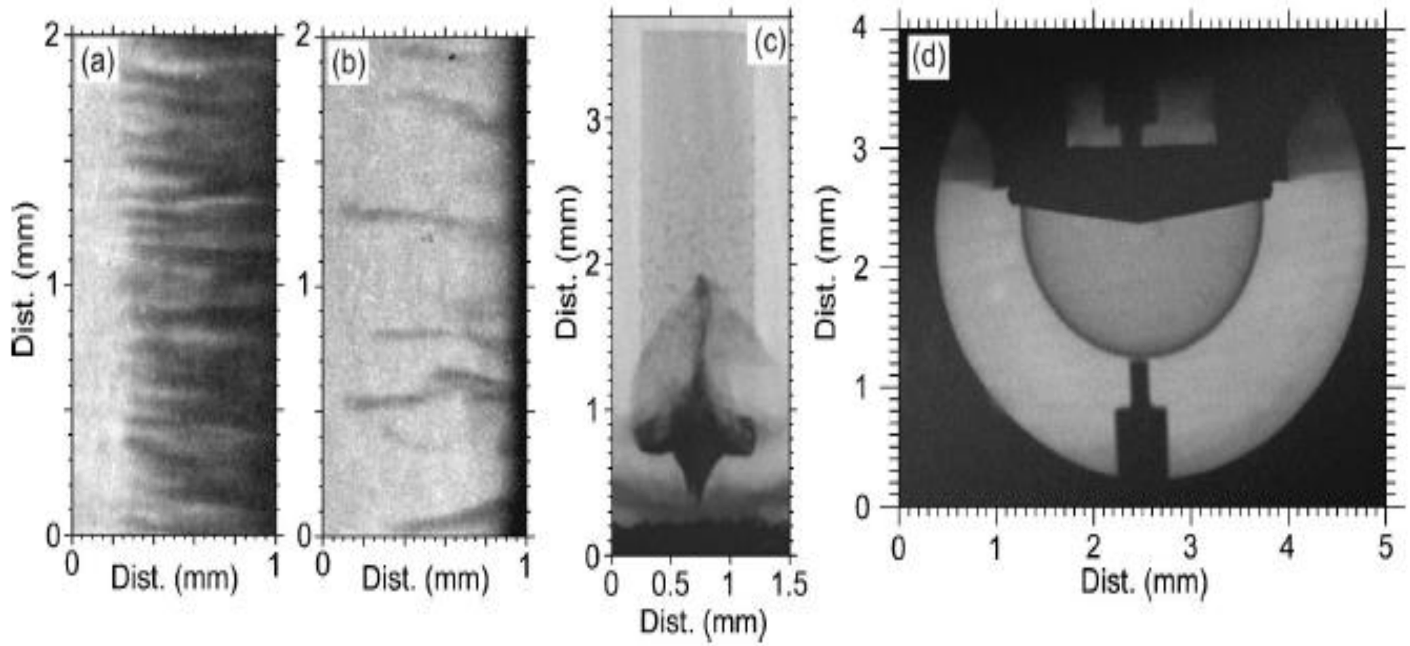

FIG. 7. (a) Example 1.865 keV radiograph of a wire-array *z*-pinch implosion (test z1100), showing an expanded view of the edge of the wire array shortly after the start of motion. (b) Example 1.865 keV radiograph of a wire-array *z*-pinch implosion (test z1050), showing an expanded view of the original edge region of the wire array. Due to the nonuniform nature of the implosion, horizontal "fingers" of mass remain near the original wire positions even though the bulk of the mass has propagated several mm radially inward. (c) Example 6.151 keV radiograph of a hydrodynamic jet experiment (test z1264) similar to those in Ref. 7. (d) Example 6.151 keV radiograph showing the implosion of a 3.02 mm hemispherical capsule shortly after the start of motion (test z1279).

D.B. Sinars et al. Rev. Sci. Instrum. 75, 3676 (2004)

Using X-ray monochromatic backlighting in High Energy Density Physics investigations (LULI Lab, France)

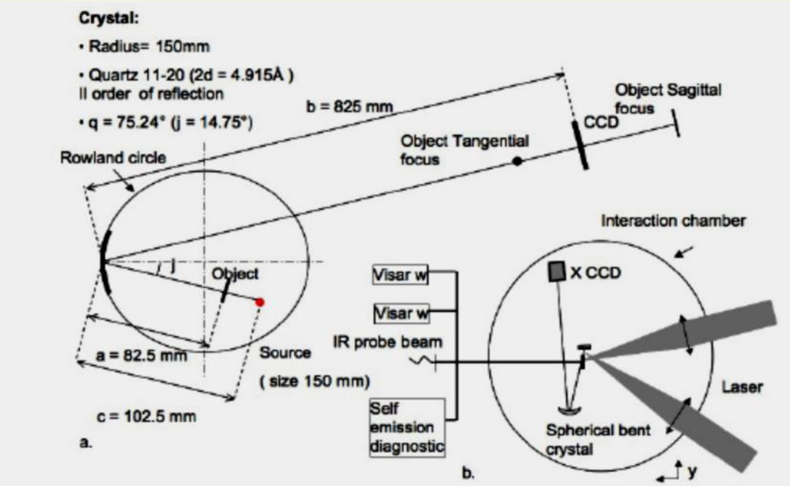

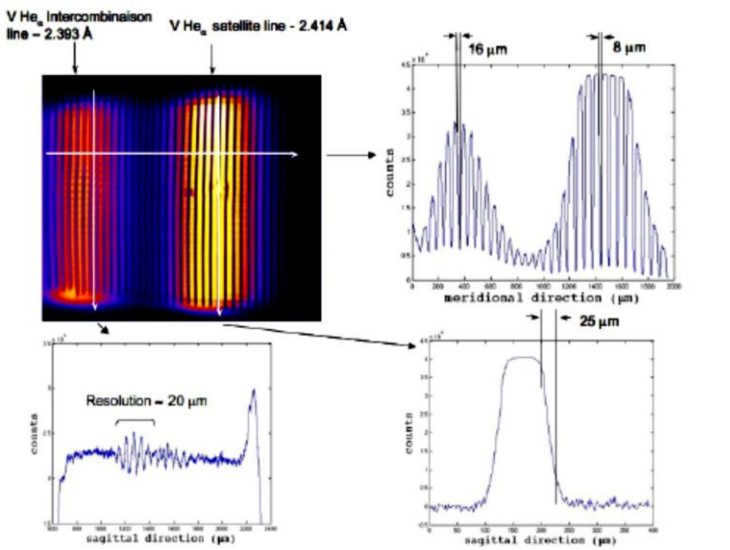

FIG. 2: Monochromatic image of a 400lpi gold grid in the backlighting scheme see figure 1.b. The densitograms of the image in the sagittal and meridional direction at 2.393Å and at 2.414Å are also presented. The hole in the grid refer to the target chamber center.

M. Koenig et al.

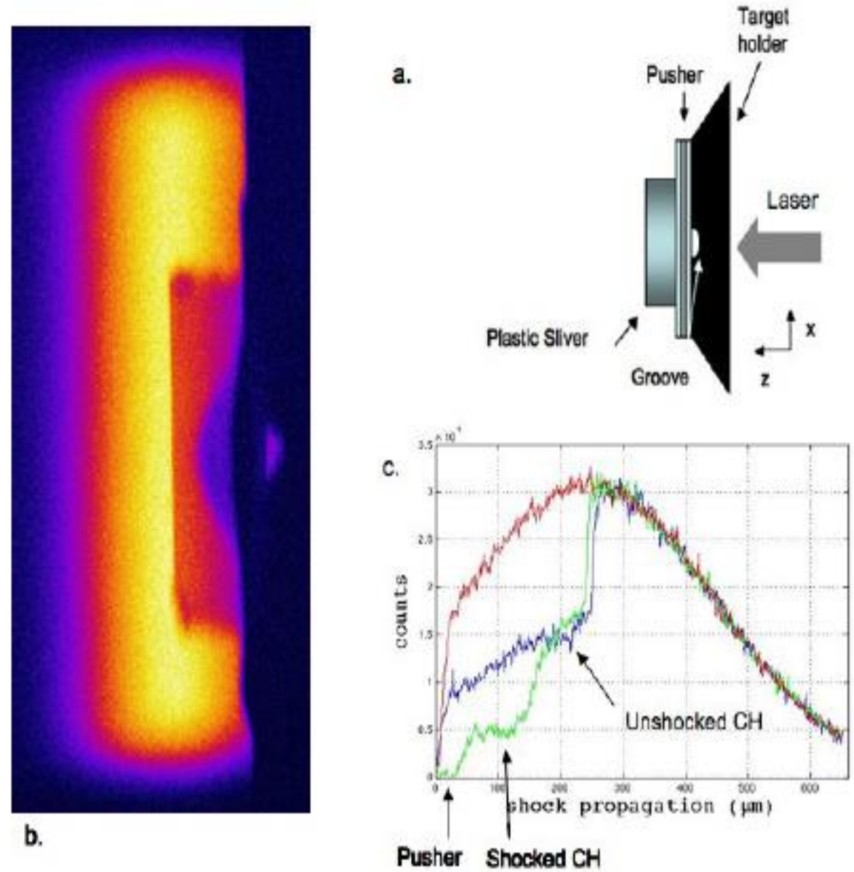

FIG. 3: (a) The target is composed by a pusher, a three layer target (10μm CH-10μm Al- 10μm CH) and, by a plastic sliver (415μm in the radiographic direction). (b) X ray shadowgraphy of the shock propagation in CH. (c) Line profile of the spectral line at 2.414Å (red, I_0), of the unshocked CH (bleu line) and of the shocked plastic (green line, I).

Monochromatic self imaging with spherically bent crystals

Two layer Al Bremsstrahlung and Ti Kα images give angle of the electron beam relative to laser axis

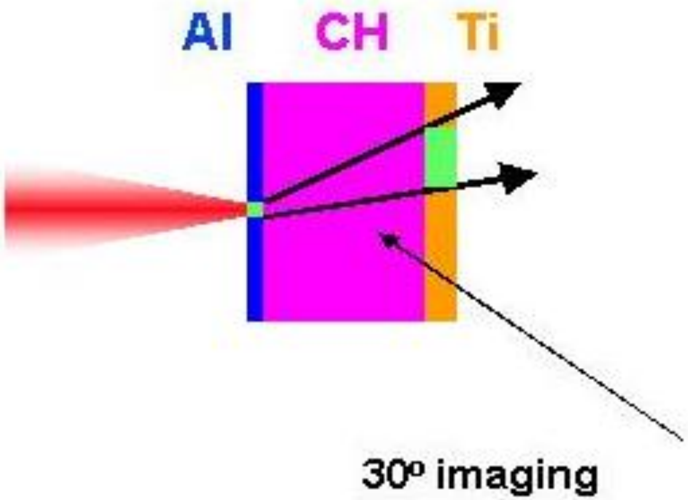

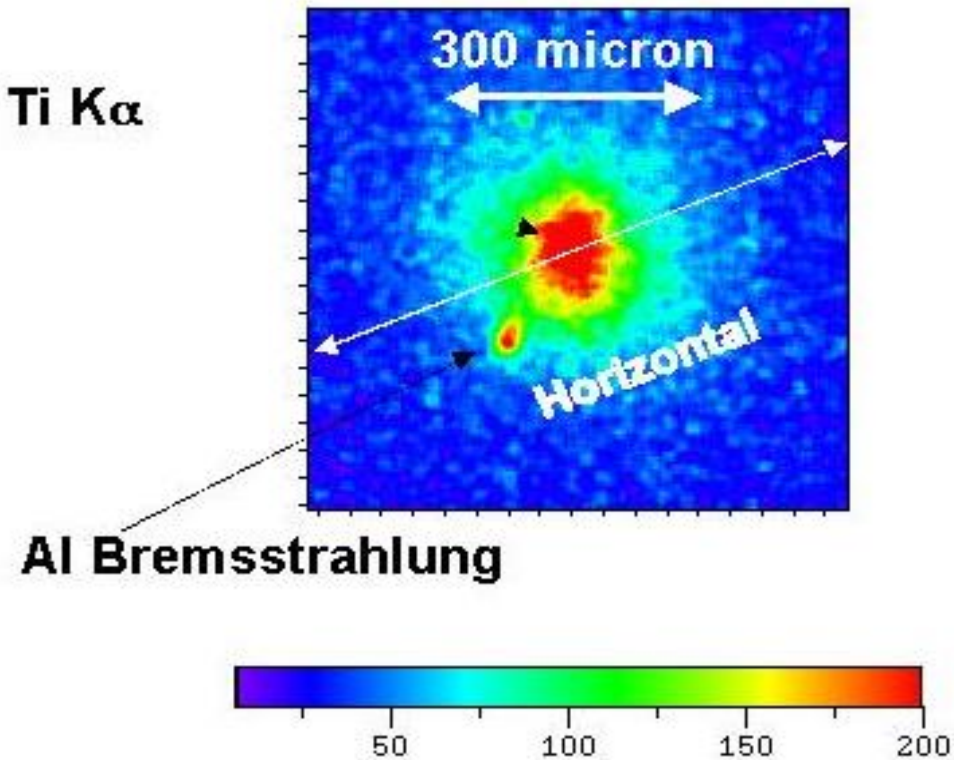

Electron beam is typically off axis

R.B. Stephens et al., PRE, 69, 066414 (2004)

Monochromatic phase - contrast image of biological object

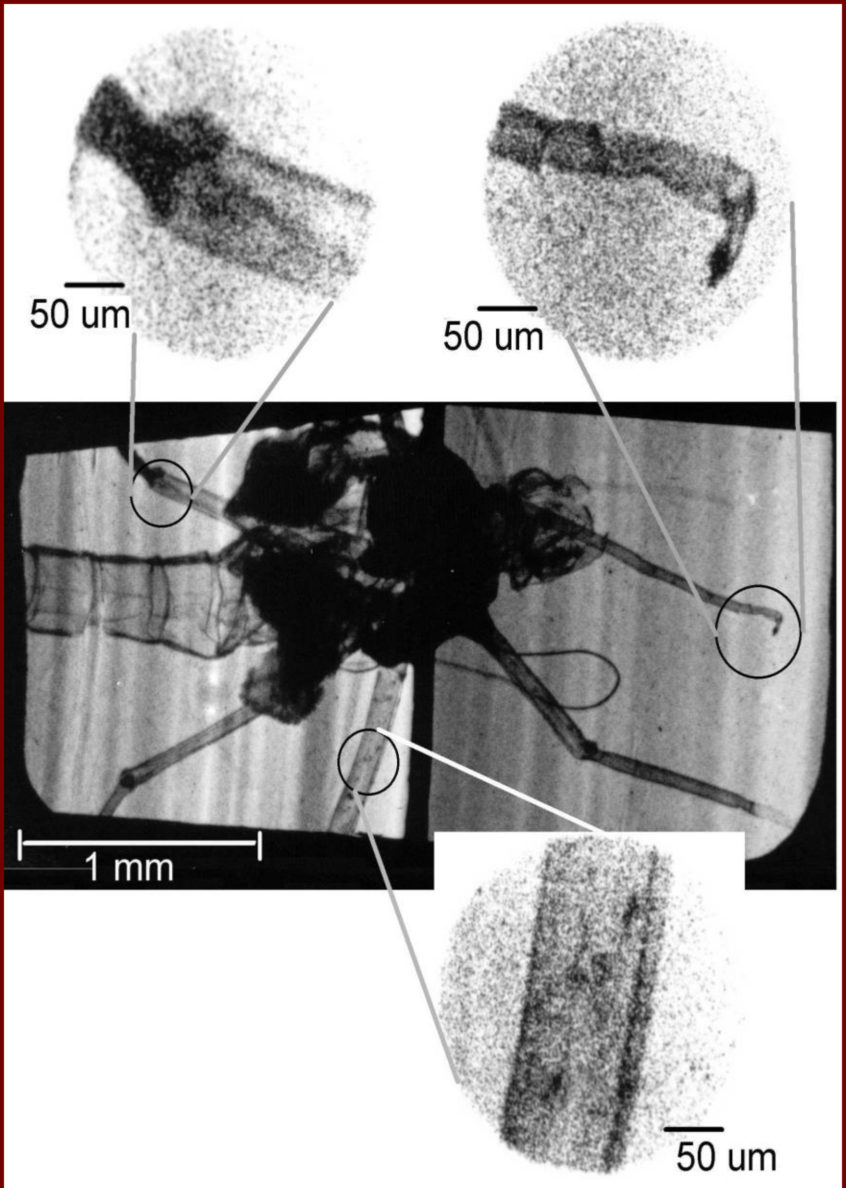

XeCl laser (1.3 J, 10 ns)

Target: Ni+Cr

Wavelength - 14.1 Å

Crystal : Mica, spherical

R = 80 mm,

(I order of reflection)

Bragg angle Θ = 45°

L'Aquila University,
ENEA, Frascati, Italy

Ref.: M.Sanchez del Rio et al., RSI ,**72** (8), 3291-3303 (2001);

T. Pikuz et al.,LPB ,**19**, 285-293 (2001)

Summary

Focusing spectrometers with spatial resolution (FSSR) allow to have:

- **High spectral resolution** $\lambda/\Delta\lambda$ **up to 10 000**
- **Wide energy range: (0.6 ÷ 14) keV for mica crystals**

  (1.45 ÷ 15) keV for quartz crystals
- **High luminosity**
- **High spatial resolution in the sagittal direction (up to 10 μm)**
- **Compact design, flexibility for mounting in different experimental vacuum chambers**

X-ray monochromatic backlighting with spherically bent crystals allows:

- **High spatial resolution ~ 2 μm in the field of view 500 μm²**

  ~ 10 μm in the field of view 4.5 x 20 mm²
- **Large field of view**
- **Good monochromaticity ($\Delta\lambda/\lambda = 10^{2} – 10^{-4}$)**
- **Rejection of background radiation**

SPECTR-W^3 ONLINE DATABASE ON ATOMIC PROPERTIES OF ATOMS AND IONS

- Ionization potentials
- Energy levels
- Spectral lines
- Bibliography
- Collision data

Internet site

http://spectr-w3.snz.ru

Available from September 2002

Welcome!

Projects ISTC # 1785 and # 3504